Hydrogeochemical controls on brackish groundwater and its suitability for use in hydraulic fracturing: The Dockum Aquifer, Midland Basin, Texas

Francisco R. Reyes, Mark A. Engle, Lixin Jin, Michael A. Jacobs, and Jasper G. Konter

ABSTRACT

To better understand controls on the origin and evolution of brackish groundwater, the hydrogeochemistry of brackish groundwaters was studied within the Triassic Dockum Group across the Midland Basin in Texas. The suitability of Dockum Aquifer water for use in hydraulic fracturing fluid was examined because the area overlies the largest and most productive tight oil province in the United States. Groundwater generally flows southward and eastward across the basin. Transmissivities indicate that water yield from the Dockum Aquifer is mixed. Higher salinity (up to ~100 g/L), group I water is found mainly in the center and western parts of the basin; chemistry of these meteoric waters is controlled by water–rock interaction with salinity increasing along its flow path via dissolution of halite and anhydrite, followed by salinity-enhanced carbonate dissolution and/or cation release from clays. Along the down-gradient basin margins, lower salinity (<7.5 g/L), group II waters of various ion compositions are more commonly found. Group II waters are also meteoric but from local recharge including downward flow from the Edwards–Trinity or other aquifers. Despite having lower salinity, the water in the down-gradient southern and eastern margins of the basin can exceed acceptable SO_4 limits for cross-linked gel fluids. Generally, the majority of the water in the basin is suitable for use with slick-water hydraulic fracturing. Findings from this research provide important information on the complex controls on the chemistry of brackish groundwater and their potential beneficial uses in the oil and gas industry.

Manuscript received September 21, 2017; provisional acceptance January 24, 2018; revised manuscript received May 15, 2018; final acceptance June 18, 2018.

DOI:10.1306/eg.01241817017

AUTHORS

FRANCISCO R. REYES ~ *Eastern Energy Resources Science Center, US Geological Survey, Reston, Virginia 20192; present address: Department of Geological Sciences, University of Texas at El Paso, El Paso, Texas; f.ruben.reyes@gmail.com*

Francisco R. Reyes is a former graduate student who graduated in 2014 with a master's degree in geology from the University of Texas at El Paso. His past academic interest and research was in groundwater origin and geochemical controls in both surface and groundwater.

MARK A. ENGLE ~ *Eastern Energy Resources Science Center, US Geological Survey, Reston, Virginia; Department of Geological Sciences, University of Texas at El Paso, El Paso, Texas 79968; engle@usgs.gov*

Mark A. Engle is a geochemist and hydrogeologist who has worked for the US Geological Survey for more than a decade. His interests include the origin and composition of brackish and saline waters coassociated with hydrocarbons. He is the corresponding author of this paper.

LIXIN JIN ~ *Department of Geological Sciences, University of Texas at El Paso, El Paso, Texas 79968; ljin2@utep.edu*

Lixin Jin is an associate professor in the Department of Geological Sciences at the University of Texas at El Paso. Her research focuses on the complex interaction of water, air, biota, and rocks in natural and managed ecosystems.

MICHAEL A. JACOBS ~ *Pioneer Natural Resources, Midland, Texas 79705; Michael.Jacobs@pxd.com*

Michael Jacobs is a hydrogeologist with Pioneer Natural Resources where he has been involved in remediation of oil field environmental issues for the past 20 years. His current role at Pioneer is corporate remediation advisor, and he is responsible for Pioneer's legacy remediation sites throughout the United States.

JASPER G. KONTER ~ *Department of Geology and Geophysics, University of Hawaii at Manoa, Honolulu, Hawaii 96822; jkonter@hawaii.edu*

Jasper G. Konter is a geochemist, formerly at the University of Texas at El Paso, and presently at the University of Hawaii at Manoa. His interests include using isotopic compositions to study processes of the Earth's interior from the crust into the mantle.

ACKNOWLEDGMENTS

This research was funded by the US Geological Survey (USGS) Energy Resources Program (Walter Guidroz, program coordinator). Additional salary support for Francisco R. Reyes was provided by a National Science Foundation GK12 program through the University of Texas at El Paso (UTEP). Pioneer Natural Resources, Apache Corporation, and Crown Quest Resources provided access to wells, cuttings, and insight into local geology. Baltazar Franco (Etech Environmental and Safety Solutions, Inc.) assisted with groundwater sampling, and Manny Sosa and Sandra Garcia (both UTEP) helped with chemical analyses. Helpful feedback on previous versions of this manuscript was provided by Peter McMahon and Jenna Shelton (both USGS) and two anonymous journal reviewers. Use of trade, firm, or product names is for descriptive purposes only and does not imply endorsement by the US government.

INTRODUCTION

Over the last decade, there has been rapid development for the extraction of hydrocarbons from continuous reservoirs, such as shale gas and tight oil. Much of this oil and gas development has occurred in arid and semiarid regions, including oil-producing shales and other lower permeability reservoirs in the Permian Basin (Texas and New Mexico), the Bakken Formation (North Dakota and Montana), the Niobrara Formation (Wyoming, Colorado, and Nebraska), and the Woodford Shale (Oklahoma and Texas). One known impact from hydrocarbon development is the quantity of water used for drilling and hydraulic fracturing, which can exceed 10,000 m^3 (~63,000 bbl) per well (Gallegos et al., 2015; Scanlon et al., 2017). Although the volume of water used in hydraulic fracturing is small relative to that used for irrigated agriculture (Nicot and Scanlon, 2012), it further intensifies debate over hydrocarbon development in arid and semiarid regions. One pathway to allow for continued oil and gas development while reducing impacts to freshwater resources is the use of brackish groundwater (defined by a total dissolved solids [TDS] concentration of 1–10 g/L) for drilling and hydraulic fracturing operations. To that end, agencies such as the US Geological Survey (USGS) (Stanton et al., 2017) and the Texas Water Development Board (2017) are assessing quality and quantity of brackish groundwater for multiple potential uses. Despite these efforts, relatively little work has been done to understand the hydrogeochemistry of brackish groundwaters, and knowledge about the quality of brackish groundwater relative to requirements for fracturing fluid chemistry is lacking. This is partially because brackish groundwaters typically occur below freshwater sources but above oil and gas reservoirs in a zone where there is little reason to install wells and collect water samples.

This effort examines the hydrogeochemistry of brackish groundwater in the Dockum Aquifer, overlying the eastern half of the Permian Basin in Texas, including the Midland Basin and surrounding carbonate shelves (Figure 1). As of February 2018, the Permian Basin is the single-largest source of tight oil in the United States, producing nearly 3 million bbl of oil per day (US Energy Information Administration, 2018). Increased use of hydraulic fracturing, a reservoir stimulation method used to maximize production from hydrocarbon wells by increasing permeability and porosity, has led to an increase in associated water consumption for hydrocarbon development in the Permian Basin (Scanlon et al., 2017). Using 2011 data, Nicot et al. (2012) estimated that 30% or more of the water for hydraulic fracturing used in the Permian Basin is brackish, although the source of these waters was not indicated. No attempt has been made to investigate the suitability of this water for various types of fracturing fluids across the play area. Moreover, relatively little is known about the geochemical controls and the evolution of water in the Dockum Aquifer in this region, making it an ideal location for better understanding of brackish groundwater systems. By examining the chemistry and distribution of water in the Dockum Aquifer, this effort

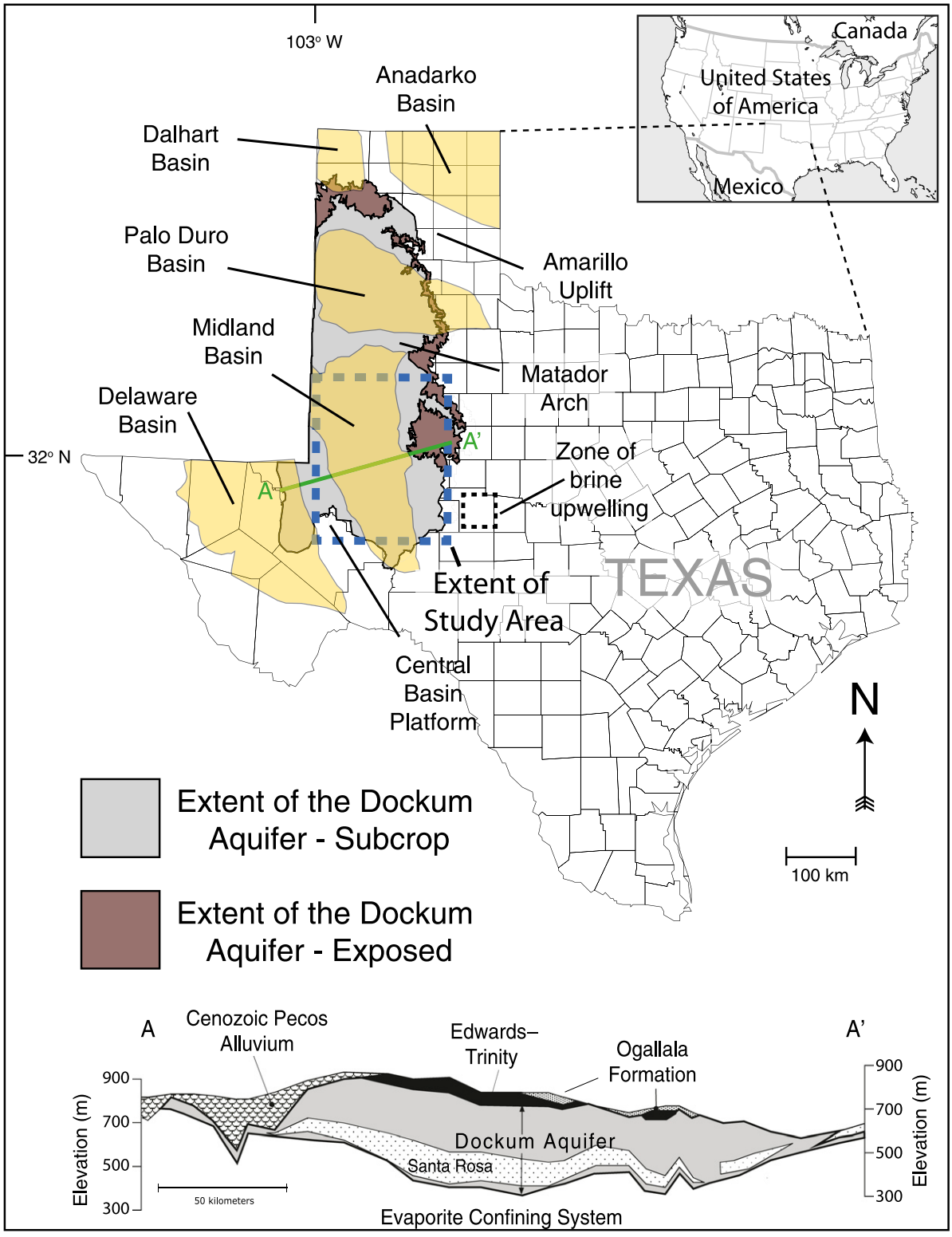

Figure 1. Map showing extent of the Dockum Aquifer in Texas (Bradley and Kalaswad, 2003), relative to nearby hydrocarbon-producing geologic basins (Coleman and Cahan, 2012). Dashed blue line shows approximate extent of study area. Also noted is approximate zone of brine upwelling into shallow groundwater in the Concho River Watershed (Dutton et al., 1989). Hydrogeologic cross section AA' of the Upper Aquifer System through the study area modified from Bradley and Kalaswad (2003).

Era	System	Series	Group	Formation	Aquifer		Hydrogeologic Unit
Cenozoic	Quaternary			Pecos Valley Alluvium	Pecos Valley		Upper Aquifer System (UAS)
	Tertiary	Late Miocene to Pliocene		Ogallala	Ogallala		
Mesozoic	Cretaceous		Fredericksburg	Kiamichi	Edwards–Trinity (High Plains)		
				Edwards			
				Comanche Peak			
				Walnut			
			Trinity	Antlers			
	Jurassic			Not present in study area			
	Triassic		Dockum	Trujillo Sandstone	Upper unit	Dockum	
				Tecovas Formation	Lower unit		
				Santa Rosa Formation			
Paleozoic	Permian	Ochoan		Dewey Lake, Salado, Castile	Nonpotable water and hydrocarbons		Evaporite Confining System (ECS)
		Guadalupian		Multiple			
		Leonardian		Sprayberry, Dean			Deep Basin Brine Aquifer System (DBBAS)
		Wolfcampian		Wolfcamp			
	Penn. to Upper Devonian			Cisco, Canyon, Strawn, Atoka, Barnett, Mississippian, Woodford			
	Lower Devonian to Cambrian			Thirtyone, Wristen Group, Fusselman, Montoya, Simpson Group, Ellenberger, Cambrian			Deep Basin Meteoric Aquifer System (DBMAS)
Precambrian							Basement Aquitard (BA)

Figure 2. Stratigraphic chart of the Midland Basin in Texas showing major hydrogeological units. Modified from Bassett and Bentley (1982), Bradley and Kalaswad (2003), Engle et al. (2016), and references therein. Penn. = Pennsylvanian.

will examine the suitability of waters in the aquifer for use in oil and gas operations and lead to insights into the origin and evolution of brackish groundwaters.

DOCKUM AQUIFER AND REGIONAL HYDROGEOLOGY

Hydrogeology of the Midland Basin

Five major hydrogeological units (Figure 2) are present in the study area (Bassett and Bentley, 1982; Engle et al., 2016). Of greatest significance to this study are (from deepest to shallowest) the Deep Basin Brine Aquifer Systems (DBBAS), the Evaporite Confining System (ECS), and Upper Aquifer System (UAS). The DBBAS includes water-bearing units of Upper Devonian to early Permian age that include most of the shales that are exploited as tight oil reservoirs in the study area (e.g., Wolfcamp, "Cline," Barnett, and Woodford shales). Produced water from the DBBAS in the study area is Na-Cl– and Ca-Cl–type with TDS concentrations ranging 45–385 g/L (Engle et al., 2016; Saller and Stueber, 2018). The 2400–2700-m (8200–8900-ft)-thick ECS corresponds to Permian (Leonardian to Ochoan)-age rocks, including a thick sequence of evaporite minerals (including halite [NaCl], anhydrite [$CaSO_4$], sylvite [KCl], and polyhalite [$K_2Ca_2Mg(SO_4)_4 \cdot 2H_2O$]) as well as underlying limestones, shales, and sandstones. The Na-Cl– and Ca-Cl–type groundwater present in the ECS has TDS concentrations up to and exceeding 300 g/L (Bein and Dutton, 1993) and has a meteoric origin, suggesting its salinity is primarily derived from dissolution of the evaporite minerals present within the ECS (Stueber et al., 1998; Engle et al., 2016). The UAS corresponds to all water-bearing units overlying the

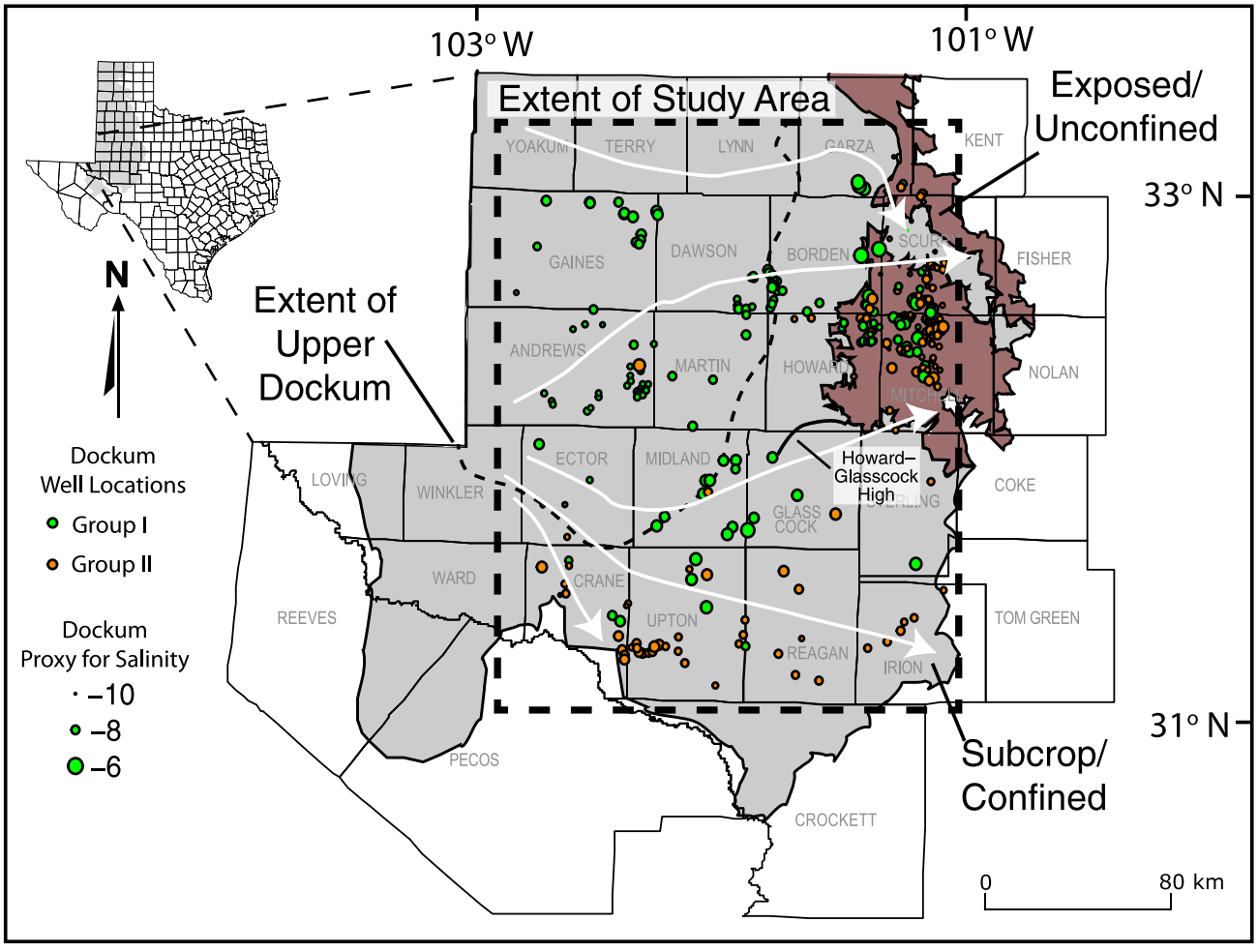

Figure 3. Map showing the spatial location of Dockum Aquifer wells used in this investigation by group, extent of the upper Dockum, extent of the subcrop Dockum, extent of the exposed Dockum, and the location of the Howard–Glasscock structural high. Groundwater flow path lines based on contoured hydraulic head shown in Figure A1 in the Appendix. Size of points scaled to isometric log-ratio proxy for salinity. Base map modified from Bradley and Kalaswad (2003).

ECS. Within the study area, thickness of the UAS is variable but generally less than 460 m. These freshwater and brackish aquifers include the Quaternary-age Pecos Valley (present only in the southwest corner of the study area), Tertiary-age Ogallala (present in the northwestern part of the study area extending as far south as southern Ector county and as far east as central Howard county; Figure 3), Cretaceous-age Edwards–Trinity (present in the southern half of the study area, extending as far north as Martin county; Figure 3), and the Triassic-age Dockum (divided into upper and lower hydrogeologic units and present throughout most of the study area; Figure 1). The Ogallala and Trinity–Edwards aquifers are the primary resources for freshwater consumption in the region (Deeds et al., 2015), although other minor aquifers such as the Dockum Aquifer are used as freshwater sources.

As a result of regional uplift and tilting related to the Laramide orogeny and Basin and Range extension (Dutton and Simpkins, 1989), groundwater flow in the UAS is generally to the south and east (Figure A1 in the Appendix). The net vertical flow in the study area is downward from the ECS into the DBBAS (Engle et al., 2016), except just down gradient of the study area (Figure 1), where ECS brines upwell into shallower aquifers in the Concho River Watershed (Dutton et al., 1989).

Geology and Hydrogeochemistry of the Dockum Aquifer

The Triassic Dockum Aquifer extends across parts of Colorado, Kansas, New Mexico, Oklahoma, and Texas (~154,000 km^2 [~60,000 mi^2], in Texas it covers

~67,600 km^2 [~26,000 mi^2]), coincident with several hydrocarbon-producing geologic basins (Figure 1). Within the study area, the Dockum Aquifer (the lowermost aquifer of the UAS) covers most of the Midland Basin but tapers out to the west, over the Central Basin Platform. Locally, the Dockum is divided into upper and lower hydrogeologic units (Figures 2 and 3) (McGowen et al., 1979). The upper Dockum pinches out further west and north than the lower Dockum (Figure 3). The lower hydrogeologic unit consists of a fine- to course-grained quartzose sandstone granule-to-pebble conglomerate, and the largely mud-rich upper hydrogeologic unit contains discontinuous sandstones, which are locally productive (Dutton and Simpkins, 1986). Zones of high water yield in the lower Dockum Aquifer are referred to as the Santa Rosa by drillers. Reported well yields for the Dockum Aquifer range from 2.7 to 13,600 m^3/day (713–3,600,000 gal/day), and transmissivity ranges from 2 to 990 m^2/day (22–11,000 ft^2/day), with a geometric mean of 41 m^2/day (440 ft^2/day) (Reyes, 2014). The aquifer has a maximum thickness of approximately 360 m (~1200 ft) in the western part of the Midland Basin, which thins eastward (30–91 m [100–300 ft]) and to the south (Bradley and Kalaswad, 2003). Much of the water in the Dockum is thought to have originated as recharge from eastern New Mexico. However, incision of the Pecos and Canadian Rivers during the Pleistocene disconnected those recharge zones to the Dockum (Dutton and Simpkins, 1989). Modern recharge to the aquifer occurs at the eastern edges of the aquifer where the unit crops out, and downward leakage comes via flow from the overlying aquifers (Ogallala, Edwards–Trinity, and the Pecos Valley) (Bradley and Kalaswad, 2003; Ewing et al., 2008; Deeds et al., 2015).

The Dockum Aquifer produces groundwater ranging from freshwater (<1 g/L TDS) to saline (>10 g/L TDS), with the majority being brackish (1–10 g/L TDS). Bradley and Kalaswad (2003) estimated that the Dockum Aquifer in Texas (from the panhandle to the northern part of Pecos county) contains 2.3×10^{11} m^3 (6.0×10^{13} gal) of water. Of that, roughly 60% was estimated to be less than 5 g/L TDS, 15% was 5–10 g/L TDS, and the remaining quarter was greater than 10 g/L TDS. Municipal and agricultural uses for Dockum Aquifer water are fairly limited because of salinity hazards (Dutton and Simpkins, 1986) and naturally occurring radionuclides in excess of drinking water limits (Bradley and Kalaswad, 2001), making it an ideal candidate for other uses, such as hydraulic fracturing.

The water source, solute source, and solute distribution of the Dockum Aquifer in the study area were examined by Dutton and Simpkins (1986, 1989), Dutton (1995), and Bradley and Kalaswad (2001, 2003). These previous studies interpreted Dockum groundwater as originating as meteoric recharge from eastern New Mexico (Figure 1) during wetter periods of the Holocene and Pleistocene, flowing east across the Permian Basin (Dutton and Simpkins, 1986, 1989; Dutton, 1995). Geochemical evolution and solute source in the Dockum Aquifer is primarily controlled by water–rock interactions involving calcite ($CaCO_3$), chalcedony (SiO_2), dolomite ($CaMg(CO_3)_2$), feldspars, kaolinite ($Al_2Si_2O_5(OH)_4$), opal ($SiO_2 \cdot nH_2O$), pyrite (FeS_2), and smectite, but the exact reactions and flow paths are not well documented. The Cl and SO_4 in Dockum Aquifer groundwater are hypothesized to be sourced from either (1) dissolution of underlying Permian-age halite and/or anhydrite or (2) mixing with connate Cretaceous seawater or associated evaporite minerals from marine transgression, which deposited much of the Edwards–Trinity (Dutton and Simpkins, 1986), but this has not been re-examined given newer studies of basinal hydrogeology (Engle and Blondes, 2014; Engle et al., 2016; Saller and Stueber, 2018).

METHODS

The majority of chemical and hydrologic data used in this investigation were taken from other sources. Midland Basin Dockum water elemental chemistry ($N = 277$) and hydrology data were taken from the Texas Water Development Board (2014) groundwater data website. In the case of this current research, information identifying which unit of the Dockum Aquifer was screened by the sampled wells was generally unavailable. In instances in which multiple data were available for an individual well, only the most recent data were used. Data for the composition of waters from oil and gas wells ($N = 1349$) were taken from Version 2.2 of the USGS National Produced Waters Geochemical Database (Blondes et al., 2016b) and from ($N = 39$) Engle et al. (2016). Constituents for which more than 50% of the entries were reported below an instruments detection limit were not used, and entries in which charge imbalance was greater than 15% were excluded. Isotope data for water samples in the study area were taken from Dutton and Simpkins (1986),

Stueber et al. (1998), Coplen and Kendall (2000), Bumgarner et al. (2012), and Engle et al. (2016). Mineral $^{87}Sr/^{86}Sr$ ratio data for mineral sources were taken from Hovorka et al. (1993) and Register and Brookins (1980).

An additional 29 groundwater samples from wells completed in the Dockum Aquifer (all Santa Rosa wells from the lower Dockum) and 6 groundwater samples from Edwards–Trinity aquifer from the study area (Figure 3) were also collected. Samples were collected using dedicated pumps from wells that were purged at least three well volumes. Additionally, pH, conductivity, oxidation reduction potential, and temperature had to reach stability for at least 5 min, as measured using a flow-through cell prior to sample collection. Separate sample aliquots (all filtered to <0.45 μm) were collected from each well: (1) acidified (Optima™ grade HNO_3) water for cations and $^{87}Sr/^{86}Sr$; (2) unpreserved water for anion concentrations, alkalinity measurements, and δ^2H, $\delta^{18}O$, and $\delta^{34}S$ in SO_4 (in some samples); and (3) unpreserved water for dissolved organic carbon (DOC). Approximately 25% of samples analyzed in this study were collected in the field by a third party using prelabeled bottles, which were acidified upon arrival at the University of Texas at El Paso (UTEP).

Concentrations of major and minor cations (B, Ba, Ca, Fe, K, Li, Mg, Na, and Sr) were determined using a Perkin Elmer Optima 5300 inductively coupled plasma-optical emission spectrometer (ICP-OES) in the Department of Geological Sciences at UTEP. Anion concentrations (Br, Cl, NO_3, and SO_4) were determined on a Dionex ICS-2100 ion chromatograph in the Department of Geological Sciences at UTEP. The DOC content was analyzed at the USGS Energy and Environmental Laboratory in Reston, Virginia, on a Shimadzu TOC-VCPH. Alkalinity was determined from gran titration using standardized concentrations of HCl on a Mettler Toledo DL15 auto-titrator in the Department of Geological Sciences at UTEP. Quality assurance and quality control samples such as matrix spikes, standard reference materials (USGS M-178, USGS M-182, and USGS T-143), field and laboratory replicates, and field and laboratory blanks were used in all analyses for each batch of samples. All samples exhibited a charge balance error of less than 10%, and the percent recovery for matrix spikes and reference materials was within ±15% for all constituents reported. Stable isotope compositions of hydrogen and oxygen in water were analyzed at the USGS Reston Stable Isotope Laboratory in Virginia. The data were converted from an activity to a concentration basis using the method of Sofer and Gat (1972, 1975). Stable isotope measurements of sulfur in SO_4 was performed for 11 Dockum samples and 6 Edwards–Trinity samples by the University of Arizona Environmental Isotope Laboratory. Saturation indices for minerals for each of the samples were computed using PHREEQC (Parkhurst and Appelo, 1999). For samples with an ionic strength greater than 0.3, the PHRQPITZ database was used, which includes Pitzer-based activity coefficients, and the remaining mineral saturations were calculated using a Debye–Hückel activity model.

Sequential extractions of two Dockum rock samples (outcrop sample of Trujillo Sandstone from Scurry County, Texas, and a cutting sample of the Santa Rosa Formation collected at a depth of approximately 400 m [~1300 ft] in Martin County, Texas) were conducted. The samples were reduced to less than 2-mm aggregates, using multiple passes through a jaw crusher that had been precleaned with 18.2 MΩ/cm water and dried in a drying oven at approximately 50°C. Following Jacobson et al. (2003) and Spivak-Birndorf et al. (2012), approximately 10 g of dried sample was reacted with 30 ml of deionized (18.2 MΩ/cm) water (water-soluble fraction; shaken for 15 min), then 10 ml of 4 M acetic acid (carbonate-bound fraction; shaken for 6 hr), and finally 10 ml of 1 M HCl (clay- and oxide-bound fraction; shaken for 6 hr). Between each extraction, samples were centrifuged at 1500 revolutions per minute for 10 min, and the fluid was removed using a syringe. Concentrations of Sr in each fraction were measured via ICP-OES, and Sr isotopes were analyzed as described below. Quantitative mineral analysis of these two samples was performed via x-ray diffraction by the USGS Central Energy Resources Science Center in Denver, Colorado.

Prior to analysis of Sr isotopes ($^{87}Sr/^{86}Sr$) in either water samples or sequential extraction fluids, column chemistry using Eichrom® Sr resin was performed to separate and purify at least 3–5 μg of Sr from the sample matrix. Each column chemistry run was performed with a blank, standard reference material (USGS EN-1 standard; all measurements [0.70917 ± 0.00001] were close to accepted value of 0.70917) and either a laboratory or field duplicate. After separation, Sr isotopes were measured on a Nu Plasma multi-collector inductively coupled plasma mass spectrometer at the Center for Earth and Environmental Isotope Research, Department of Geological Sciences at UTEP. The resulting $^{87}Sr/^{86}Sr$ values (N = 40 ratios, 2-cycle

multidynamic mode) were corrected online for interferences from ^{87}Rb and ^{86}Kr and for mass-based fractionation using $^{86}Sr/^{88}Sr = 0.1194$ (Konter and Storm, 2014). Data were corrected using a standard-sample bracketing method, wherein the values for reference material SRM 987 were adjusted to match the accepted $^{87}Sr/^{86}Sr$ value of 0.71025. External precision of the USGS EN-1 secondary standard over the course of runs was 0.000015 (two standard deviations). It should be noted that only half as many ratios are collected here as described in Konter and Storm (2014) because the resulting precision is sufficient for this work.

Chemical data, including concentrations of ions in water, are compositional in that they are parts of a total sum. Compositional data, as has been known for decades, need to be treated in a special manner to avoid problems such as induced correlations and potentially incorrect interpretation. Previous works have shown that even data in units such as millimoles per liter or milligrams per liter are compositional (Buccianti and Pawlowsky-Glahn, 2005; Engle and Rowan, 2013) and that, in particular, saline waters (>10 g/L TDS) are susceptible to spurious correlations and incorrect interpretations, which can result from the use of raw concentration data (Engle and Blondes, 2014; Engle et al., 2016). Intuitively, this is because the amount of water per given volume or mass (depending on units) varies tremendously between the samples. Because the total sum of constituents, including water, adds to a constant, the other constituents are artificially constrained to have a positive correlation, even if they have no actual association. Multiple examples of how drastically results can differ between the two approaches can be found elsewhere (Otero et al., 2005; Engle and Rowan, 2013; Engle and Blondes, 2014; Engle et al., 2016), and explanations for which groups of elements are most impacted by these differences are known (Blondes et al., 2016a), so such a comparison will not be repeated here. Instead, this effort will rely on conversion of concentration data for D (number of constituents) to D – 1 (number of isometric log ratios [ilr]) through the use of a singular binary partition (SBP). Developing an SBP, as will be shown later, involves coding different parts as +1, –1, or leaving them blank, as per the user's preference, using a set of rules described by Egozcue and Pawlowsky-Glahn (2005). The corresponding ilr coordinates or balances (z_i) are calculated by

$$z_i = \sqrt{\frac{r_i s_i}{r_i + s_i}} \ln \frac{\left(\prod x_j\right)^{\frac{1}{r_i}}}{\left(\prod x_l\right)^{\frac{1}{s_i}}} \quad for \;\; i = 1, \ldots, D-1 \qquad (1)$$

where r_i and s_i are the number of parts coded with +1 and –1, respectively, and x_j and x_l are the constituents in units of millimoles per liter (e.g., ions or elements in the composition or subcomposition) coded with +1 and –1, respectively. For any given compositional data set, the SBP can be arranged in different ways, allowing for the data analyst to rearrange the partitions to create ilr balances that best help with interpretation. For example, in a simple two-part composition (say Na and Cl), the single-resulting ilr balances are either

$$z_1 = \sqrt{\frac{1}{2}} \ln \frac{[Na]}{[Cl]}$$

where Na is coded with +1 and Cl is coded with –1 or

$$z_1 = \sqrt{\frac{1}{2}} \ln \frac{[Cl]}{[Na]}$$

where Na is coded with –1 and Cl is coded with +1. For mathematical reasons, conversion of isotopic data (either straight ratios or delta notation) provides little change in plotting results (Blondes et al., 2016a) and are thus kept in their original units.

Table 1. Singular Binary Partition for the Seven-Part Subcomposition (Ca, Cl, HCO_3+CO_3, H_2O, Mg, Na, SO_4)

Partition	Ca	Cl	HCO_3+CO_3	H_2O	Mg	Na	SO_4	r	s	Meaning
1	+1	+1	+1	–1	+1	+1	+1	6	1	Salinity proxy
2	+1	–1	–1	N/U	+1	+1	–1	3	3	Anions versus cations
3	+1	N/U	N/U	N/U	+1	–1	N/U	2	1	Alkaline earth versus alkalis
4	+1	N/U	N/U	N/U	–1	N/U	N/U	1	1	Ca versus Mg
5	N/U	+1	–1	N/U	N/U	N/U	–1	1	2	Cl versus alkalinity and SO_4
6	N/U	N/U	+1	N/U	N/U	N/U	–1	1	1	Alkalinity versus SO_4

Abbreviations: N/U = constituent not used in the partition; r = number of +1s in balance; s = number of –1s in balance.

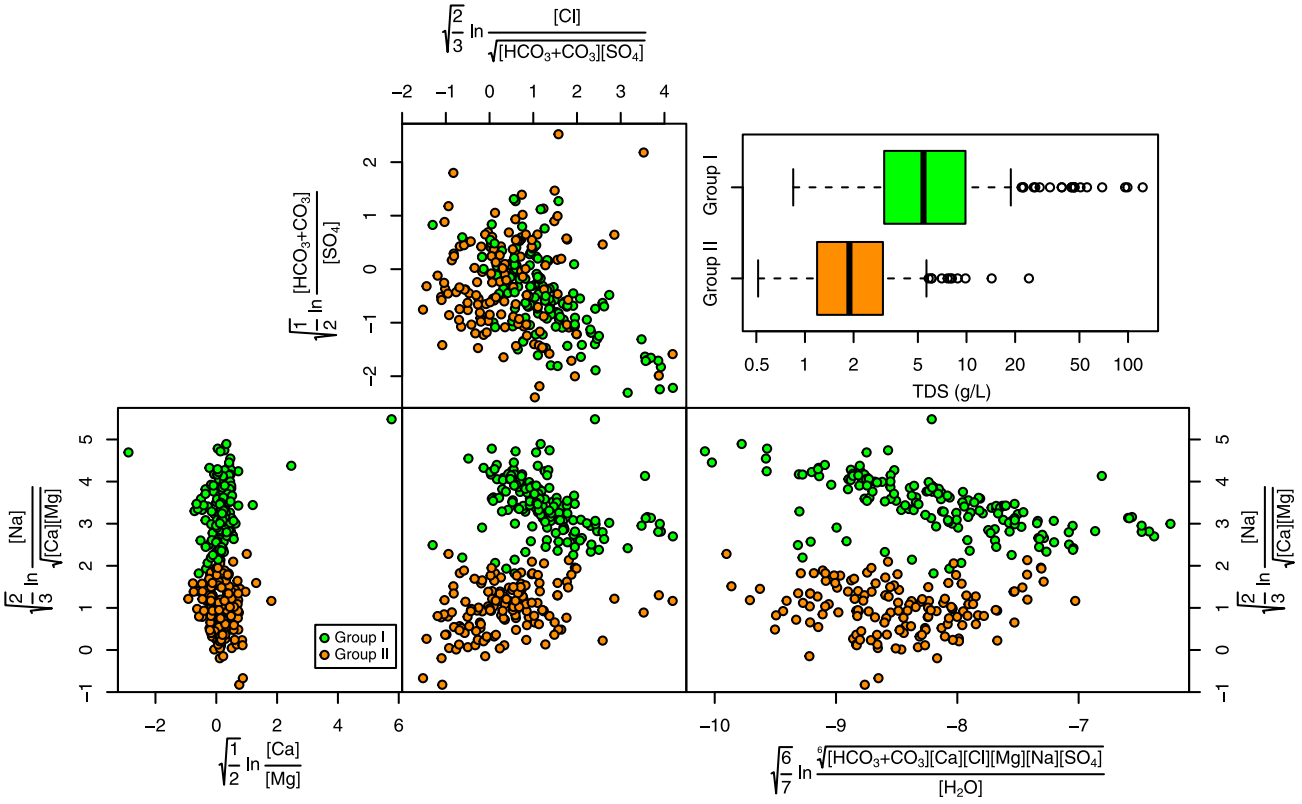

Figure 4. Plot of isometric log-ratio transformed coordinates for a seven-part subcomposition containing all major ions and water. The leftmost panel shows the relative abundance of cations, the topmost panel shows the relative abundance of anions, the center panel shows project coordinates for each point from the anions and cation panels, and the rightmost panel shows the relative abundance of the cations versus the geometric mean of the major ions versus water content. The isometric log-ratio coordinates are derived using the singular binary partition in Table 1 and equation 1. TDS = total dissolved solids.

DOCKUM AQUIFER HYDROGEOCHEMISTRY RESULTS AND INTERPRETATION

Major Ion Chemistry

To investigate the major ion chemistry of Dockum Aquifer water samples (see Table A1 in the Appendix for the geochemical data for 35 samples collected as part of this study), a 7-part subcomposition consisting of 6 ions (Ca, Cl, HCO_3+CO_3, Mg, Na, and SO_4) and water content (calculated as the difference between the sample density and TDS) in units of millimoles per liter was arranged in a SBP following the rules of Egozcue and Pawlowsky-Glahn (2005). To avoid the presence of zeros, which can prevent conversion of data into ilr balances, CO_3 and HCO_3 data were amalgamated into a single part (HCO_3+CO_3). Potassium was excluded given poor data coverage and low concentration. The resulting six balances were arranged in a way to provide meaningful interpretation (detailed in Table 1) and allow for transformation of the data into six ilr-transformed variables (using the SBP and equation 1). For instance, the first balance ratios the geometric mean of all of the ions in the subcomposition to the water content (Table 1), serving as a proxy for salinity. Several of the resulting ilr variables were plotted against one another, producing a figure similar to a Durov diagram (Figure 4). The leftmost panel of this plot examines the relative abundance of the cations, the top panel shows the relative abundance of anions, the center panel projects points from the anion and cation panels, and the rightmost panel explores the "salinity" balance (i.e., balance 1) against the alkali versus alkaline earth content of the samples. Reyes (2014) and Engle et al. (2017) previously separated the data into two geochemical groups, group I and group II, based upon separation between the two in principal component analyses. We have used a nearly identical grouping but simplified the classification based upon a molar Na/Ca ratio of 12.5:1. The *x*-axis of the leftmost panel shows

Table 2. Reordered Singular Binary Partition for the Seven-Part Subcomposition (Ca, Cl, HCO_3+CO_3, H_2O, Mg, Na, SO_4)

Partition	Ca	Cl	HCO_3+CO_3	H_2O	Mg	Na	SO_4	r	s	Meaning
1	+1	+1	+1	−1	+1	+1	+1	6	1	Salinity proxy
2	+1	−1	−1	N/U	−1	−1	+1	2	4	N/U
3	+1	N/U	N/U	N/U	N/U	N/U	−1	1	1	Ca versus SO_4
4	N/U	+1	−1	N/U	−1	+1	N/U	2	2	N/U
5	N/U	−1	N/U	N/U	N/U	+1	N/U	1	1	Na versus Cl
6	N/U	N/U	+1	N/U	−1	N/U	N/U	1	1	N/U

Abbreviations: N/U = constituent not used in the partition; r = number of +1s in balance; s = number of −1s in balance.

that on a log scale, the molar Ca to Mg ratio of the samples is relatively constant and fairly close to one (ratios of one produce ilr values of zero, because of the log). The *y*-axis, a comparison between Na and a geometric mean of the Ca and Mg content, varies tremendously. The vast majority of samples exhibit positive values on this axis, indicating that Na is the dominant cation (molar basis) for most Dockum Aquifer groundwater. In the anion panel (top panel), there is a substantial range along both axes, and no clear trends exist. The group I samples exhibit slightly more positive values along the *x*-axis, suggesting generally higher chlorinity relative to the group II samples. The middle panel, which projects the points from the anion and cation panel, shows a clear distinction between the two sample groups. For the group I samples, as the relative abundance of Na to Ca and Mg decreases so does the abundance of HCO_3+CO_3 and/or SO_4 relative to Cl. Most of the samples are near saturation for calcite and dolomite (Figure A2 in the Appendix), so there is little variation in concentration of CO_3+HCO_3. Thus, this trend is a result of an increase in the relative abundance of SO_4 and Cl with decreasing relative abundance of Na. By comparison, the Group II samples only have a relatively weak trend of relative Cl increasing with relative increases in Na. The rightmost panel indicates that for the Group I samples, high salinity is associated with a lower relative abundance of Na, whereas the group II samples show no obvious trends between cation abundance and salinity, except that they tend to exhibit a lower salinity that the group I samples. This relationship is supported by the difference in TDS between the two groups, as noted in the inset boxplot (Figure 3).

Ochoan-age halite and anhydrite deposits, both readily soluble salts, underlie the Dockum Aquifer in the study area (Figure 2) and represent a potential solute source. Additionally, gypsum is also present in parts of the Edwards–Trinity aquifer, which overlies the Dockum in the southern half of the study area. In an attempt to better understand contribution from the evaporites, the SBP in Table 1 was reworked to allow for molar ratios of Na/Cl and Ca/SO_4 to be contained in the balances (Table 2). Plotting ilr balances made from partitions 1 versus 5 and 1 versus 3 shows the relationships between the Na/Cl molar ratio and salinity (Figure 5) and between the molar Ca/SO_4 ratio and salinity (Figure 6), respectively. Water that dissolves halite should approach a value of zero on an ilr balance featuring the Na/Cl ratio. Similarly, water that dissolves anhydrite should approach a value of zero on a Ca/SO_4 ilr balance. In both cases, higher salinity group I Dockum Aquifer samples approach the ilr values of zero, which is similar to the composition of produced waters from the ECS, suggesting that anhydrite and halite are important salinity sources. Mass-balance calculations indicate that samples exhibiting Na/Cl and Ca/SO_4 ilr values approaching zero have dissolved up to 47.4 g (0.82 mol) of halite and 3.9 g (0.028 mol) of anhydrite per liter of groundwater. These numbers roughly match the upper end of salinity for these samples. The large amount of halite dissolved relative to anhydrite is one reason why the group I groundwater contains a higher proportion of Na relative to Ca and Mg (Figure 3). Alternatively, group II waters show little variation with respect to either Na/Cl or Ca/SO_4 ratios with increasing salinity (represented by the *x*-axis in Figures 5 and 6). The results also show that the group II samples tend to exhibit negative Ca/SO_4 ilr values and Na/Cl ilr values that can either be either positive or negative, whereas the group I samples almost exclusively have positive Na/Cl ilr values. Such differences, even in lower salinity samples, suggest that the group I and group II Dockum Aquifer groundwaters are of different origin.

Spatial mapping shows that the group II samples are primarily found along the basin margins to the south and east of the study area where the Dockum is shallow or the unit crops out and where the upper Dockum is absent (Figure 3). Conversely, group I samples are more

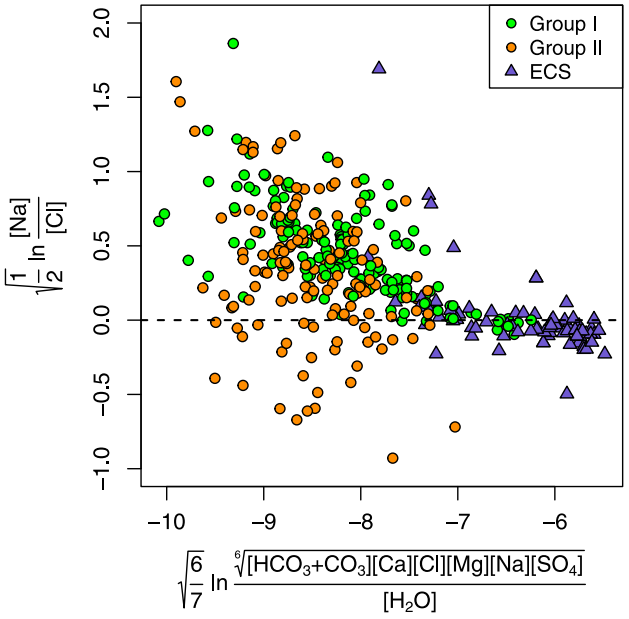

Figure 5. Plot of isometric log-ratio transformed coordinates showing the relative abundance of Na/Cl (molar) versus a proxy for salinity. ECS = Evaporite Confining System.

generally found in the up-gradient central and western parts of the Midland Basin. In general, the group I Dockum group samples were collected from deeper depths (>150 m [500 ft]) relative to those from the group II Dockum group (Figure A3 in the Appendix), and an increase in salinity with well depth ($p < 0.0001$, $r^2 = 0.263$) is observed. However, depth alone does not fully explain the large variance in TDS concentration data; Dockum groundwater can be brackish at shallow depths (e.g., 6–30 m [20–100 ft]). In samples from the northern half of the Midland Basin, TDS is about 1.7 g/L in the western-most part of the study area. Generally, dissolved constituents tend to be more concentrated toward the down-gradient part of the Midland Basin, reaching a maximum (TDS >50 g/L) near the eastern edge and southern half of the Dockum Aquifer in the study area. Samples exhibiting the highest salinity values (both in Borden and Garza counties and south and southwest of the Howard–Glasscock structural high) overlap with zones of documented postdepositional dissolution of evaporites in the underlying Permian salts (Hovorka, 1998). These same saline samples also exhibit molar ratios suggesting significant solute contribution from anhydrite and halite dissolution (Figures 5 and 6). A pattern of increasing salinity along the flow path indicates that continuous mineral dissolution is an important source of solutes in Dockum groundwaters across the Midland Basin and that the salinity proxy used in Figures 4–6 is a reasonable surrogate for geochemical maturity during groundwater transport. In the southern part of the basin, lower TDS values in Dockum Aquifer groundwater (<1.5 g/L) are found along the basin margins, roughly coincident with the extent of group II waters.

Results from geochemical modeling of saturation indices show that nearly all samples are at or near equilibrium with quartz and carbonate minerals (Figure A2 in the Appendix). As salinity increases, halite saturation increases but stays well below equilibrium, and anhydrite approaches saturation, suggesting Ca and SO_4 concentrations in Dockum Aquifer groundwaters are buffered.

Isotope Geochemistry

Stable isotopic data for oxygen and hydrogen indicate that both group I and group II waters are of meteoric origin and both data sets plot slightly below (Figure 7) the global meteoric water line. Using data for the Colorado River of Texas Edwards–Trinity aquifer, the Pecos Valley Alluvial Aquifer, and the Dockum Aquifer, the local meteoric water line (LMWL) is defined as $\delta^2H = 6.55 \times \delta^{18}O - 3.37$ (a nearly identical trend is generated without the inclusion of Dockum Aquifer samples). Within Dockum Aquifer groundwaters, group I samples are on average more enriched in ^2H and ^{18}O

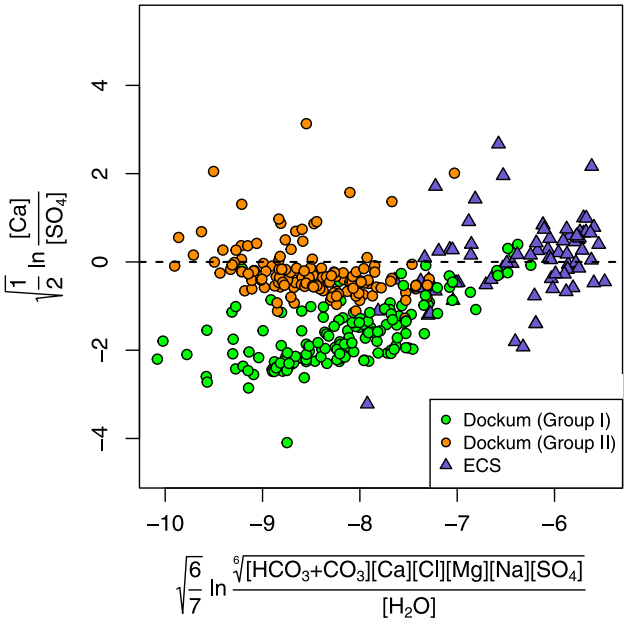

Figure 6. Plot of isometric log-ratio transformed coordinates showing the relative abundance of Ca/SO_4 (molar) versus a proxy for salinity. ECS = Evaporite Confining System.

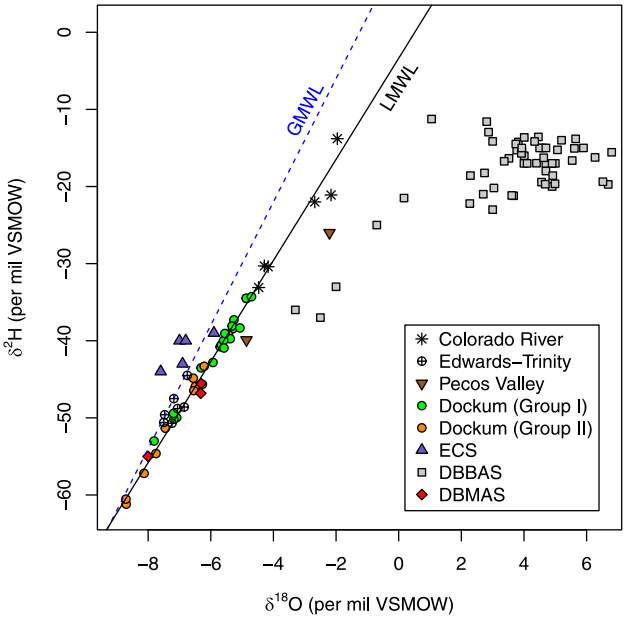

Figure 7. Plot of δ^2H versus $\delta^{18}O$ for water samples from the study area. DBBAS = Deep Basin Brine Aquifer System; DBMAS = Deep Basin Meteoric Aquifer System; ECS = Evaporite Confining System; GMWL = global meteoric water line; LMWL = local meteoric water line; VSMOW = Vienna standard mean ocean water.

relative to the lighter isotopes than group II samples (Figure 7), suggesting different recharge conditions. Average recharge temperatures were estimated from $\delta^{18}O$ data (Dansgaard, 1964), indicating that group II samples recharged under significantly cooler (Wilcoxon rank-sum test, $p < 0.01$) conditions, approximately 2°C cooler, than those from group I. Assuming that all the Dockum groundwater was recharged under the same climate, one can conclude the group II water was recharged at a higher altitude (an estimated 400 m [1300 ft] higher) than group I water. None of the Dockum Aquifer samples deviate off the LMWL toward the data for ECS (paleometeoric water) or DBBAS samples (evaporated, Late Permian seawater), suggesting no major contributions from those sources to the samples analyzed. Data from the deepest hydrogeology unit, the Deep Basin Meteoric Aquifer System, do overlap with the Dockum Aquifer samples but exist below the DBBAS and ECS (typically below 3000 m [10,000 ft]) and are unlikely to have migrated upward and bypassed the other two aquifer systems (Engle et al., 2016). This agrees with mixing calculations for $\delta^{18}O$ and Cl, showing that increasing salinity in Dockum Aquifer samples, with the exception of three samples, cannot be explained by mixing with either brines from the ECS or DBBAS or evaporation (Figure A4 in the Appendix). Three Group I samples, which occur in the eastern edge of the study area where the Dockum outcrops, do suggest input from ECS brines but were collected from hydrocarbon wells originally screened in the ECS, which had been converted to water supply wells screened in the Dockum. These three samples show no other obvious geochemical deviations from other high-salinity group I Dockum waters. Stable isotopic data for oxygen and hydrogen data from these three wells plot directly on the LMWL, away from the ECS brines and exhibit $^{87}Sr/^{86}Sr$ ratios much more radiogenic than ECS waters (Figure 8), suggesting that if they are mixed with ECS waters, the degree of mixing is small.

Data for $^{87}Sr/^{86}Sr$ were combined with ilr-transformed molar Na/Cl ratios to examine sources of Sr in Dockum Aquifer groundwaters (Figure 8). All of the samples plot away from known Sr-bearing mineral sources in the basin, including anhydrite of Guadalupian and Ochoan age, Ochoan polyhalite, and mixtures of Ochoan halite and sylvite (data from Register and Brookins, 1980; Hovorka et al., 1993). Notably, as the group I Dockum Aquifer samples approach a value of zero on the *y*-axis and their maximum salinity (Figure 4), the data approach a $^{87}Sr/^{86}Sr$ value of approximately 0.7095. Results from Figures 5 and 6 indicate that these

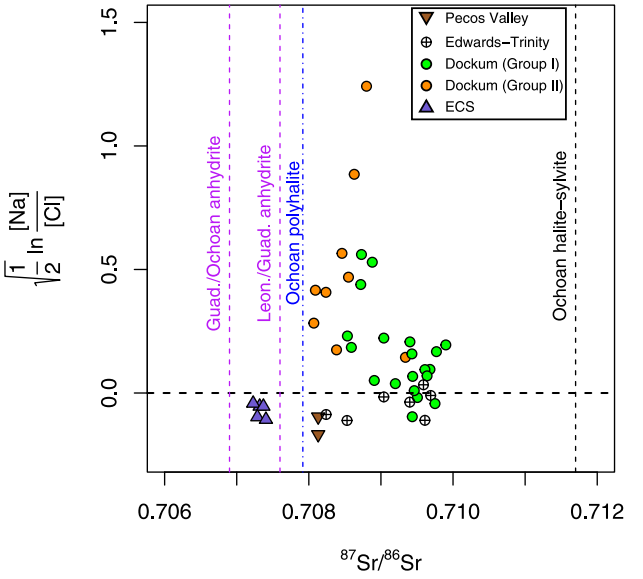

Figure 8. Plot of the isometric log-ratio transformation of the molar Na/Cl ratio versus $^{87}Sr/^{86}Sr$ for groundwater samples from the Dockum Aquifer and adjacent units. The $^{87}Sr/^{86}Sr$ ratio data for mineral sources were taken from Hovorka et al. (1993) and Register and Brookins (1980). ECS = Evaporite Confining System; Guad. = Guadalupian; Leon. = Leonardian.

Table 3. X-Ray Diffraction and Sequential Extraction Leaching Sr Concentration and $^{87}Sr/^{86}Sr$ Results from Two Dockum Rock Samples

Method	Upper Dockum (Trujillo) Outcrop Sample	Lower Dockum (Santa Rosa) Cuttings Sample	Targeted Phases
X-ray diffraction results	Quartz (54.2%), calcite (24.8%), albite (10.7%), muscovite (5.4%), kaolinite (2.8%), illite (2.0%)	Quartz (60.2%), illite (14.1%), albite (10.1%), muscovite (8.6%), calcite (6.4%), kaolinite (0.5%),	
DI leach	0.32 mg/kg; $^{87}Sr/^{86}Sr = 0.70957$	0.79 mg/kg; $^{87}Sr/^{86}Sr = 0.70920$	Water-soluble minerals (e.g., sulfates)
4 M acetic acid leach	15.5 mg/kg; $^{87}Sr/^{86}Sr = 0.70985$	32.7 mg/kg; $^{87}Sr/^{86}Sr = 0.70936$	Carbonate minerals (e.g., calcite)
1 M HCl leach	9.5 mg/kg; $^{87}Sr/^{86}Sr = 0.71008$	15.7 mg/kg; $^{87}Sr/^{86}Sr = 0.70959$	Oxides, clays

Abbreviation: DI = deionized.

same samples have been impacted by increased salinity through the dissolution of anhydrite and halite. For group I Dockum Aquifer samples that plot near the zero value on the *y*-axis in Figure 8, if we assume that all of the SO_4 (~28 mmol/L) came from anhydrite dissolution (Sr = 2404 mg/kg, $^{87}Sr/^{86}Sr = 0.70692$) and all of the Cl (~810 mmol/L) came from halite dissolution (Sr = 19.4 mg/kg, $^{87}Sr/^{86}Sr = 0.71169$), simple mass-balance end-member mixing estimates these groundwaters to have a $^{87}Sr/^{86}Sr$ value of 0.70736, far below the $^{87}Sr/^{86}Sr$ values observed and at the low end of Sr concentrations in these samples (11.3 mg/L vs. 7.8–54.3 mg/L). Notably, the limited $\delta^{34}S$ data from 11 Dockum water samples show that as salinity increases, sulfur isotopes get heavier (~10‰–15.7‰), overlapping with both the range of upper-Permian evaporites (Hovorka et al., 1993) and early-Cretaceous seawater (Claypool et al., 1980) (Figure A5 in the Appendix).

Sequential Extraction of Dockum Rock Samples

Both rock samples produced the most Sr (15.5 and 32.7 mg of Sr per kilogram of dry rock) in the 4 M acetic acid extraction (targeting carbonate phases; step 2 of the extraction) and the least amount (0.32 and 0.79 mg of Sr per kilogram of dry rock) in the water extractions (targeting water soluble phases; step 1 of the extraction), with an intermediate amount of Sr (10.0 and 15.7 mg of Sr per kilogram of dry rock) in the 1 M HCl extractions (targeting clays and oxides; step 3 of the extraction) (Table 3). Interestingly, the outcrop sample contained nearly three times more calcite (Table 3) and generated greater than two times more Ca during the acetic acid sequential extractions (Table A2 in the Appendix) than the cuttings sample but produced less Sr in all three extractions. Evidence that the acetic acid extractions primarily only released elements in carbonate minerals is supported by relatively minor release of Ba (<5 mg/kg) and Fe (<30 mg/kg) in these extractions relative to the HCl extractions (>5 mg/kg and >30 mg/kg, respectively), which primarily extracts clays and oxides (Spivak-Birndorf et al., 2012). Data for $^{87}Sr/^{86}Sr$ in the sequential extraction fluids showed little variance between samples and leaching compounds (0.70957 to 0.71008). These values are remarkably similar to the group I Dockum Aquifer samples that approach an ilr-transformed molar Na/Cl ratio value of zero in Figure 8. Such results suggest that carbonate minerals, and possibly clay and oxide minerals, within the Dockum aquifer are the primary source of Sr in these waters. Because calcite is pervasive throughout the extent of the Dockum, and geochemical modeling suggests nearly all Dockum waters are at or near saturation with calcite (Figure A2 in the Appendix), one would expect that $^{87}Sr/^{86}Sr$ ratios across the study areas would be fairly uniform instead of exhibiting the observed trend in the data. One possible explanation is dissolution of calcite in areas of high salinity because of its increased solubility in higher ionic strength solutions. Geochemical modeling (PHRQPITZ database) shows that the calcite solubility more than doubles in a 0.25 M NaCl solution (which is similar to values for some of group I Dockum Aquifer samples that approach an ilr-transformed molar Na/Cl ratio value of zero) relative to pure water (34.0 mg/L vs. 14.6 mg/L, respectively). Similarly, influx of halite-rich waters can induce Sr desorption from clay minerals (El-Assy et al., 1991). Simple mass-balance calculations indicate that an additional approximately 18 mg/L or more of Sr with an $^{87}Sr/^{86}Sr$ ratio of 0.710 (consistent with the rock sample extractions), beyond the Sr

contribution from anhydrite and halite dissolution (discussed in the Isotope Geochemistry section), would produce TDS, Sr concentrations, and $^{87}Sr/^{86}Sr$ values similar to those of the highest-salinity group I waters. Thus, Dockum waters that dissolve evaporites may induce local carbonate dissolution and/or Sr desorption from clays within the Dockum, producing an $^{87}Sr/^{86}Sr$ ratio in the water that mimics this mineral fraction, as opposed to the evaporite minerals.

CONCEPTUAL MODEL FOR DOCKUM AQUIFER HYDROGEOCHEMISTRY

Evolution and Origin of Dockum Aquifer Brackish Groundwater

Compiling information from the previous sections and insight from previous investigations, the group I Dockum Aquifer waters evolves from low-TDS (<5 g/L) water with high relative proportions of Na and SO_4 to high-salinity water with increasing proportions of Ca, Cl, and SO_4 (Figure 3) moving along the groundwater flow path from west to east and southeast (Figure 6). Notably, after development of the Pecos River Valley, recharge to the west to the Dockum in New Mexico ceased (Dutton and Simpkins, 1986, 1989). Thus, the group I waters found in deeper parts of the basin may represent groundwater that recharged prior to development of the Pecos River Valley and flowed through reactive silicates or clay in the upper Dockum unit. This flow path modified the solutes to a composition more similar to that of group I before entrance into the deeper, sandstone-rich part of the aquifer, where dissolution of evaporite minerals begins. Examination of mineralogical data for the Dockum (Table 3) and knowledge that these waters are near saturation with respect to calcite suggests that a combination of calcite dissolution

$$CaCO_3 + H^+ \rightarrow Ca^{2+} + HCO_3^-$$

and incongruent dissolution of albite ($NaAlSi_3O_8$) into kaolinite ($Al_2Si_2O_5(OH)_4$)

$$2NaAlSi_3O_8 + 2CO_{2(g)} + 11\,H_2O \rightarrow Al_2Si_2O_5(OH)_4 + 2Na^+ + 2HCO_3^- + 4H_4SiO_{4(aq)}$$

coupled with Na for Ca cation exchange on clay minerals may explain the origin of the Na-HCO_3 waters near the recharge areas in New Mexico (Figure 9). This agrees with thermodynamic stability data for Dockum waters showing control from calcite, kaolinite, and smectite (Dutton and Simpkins, 1986). The group I waters are thought to recharge from slightly lower elevations in eastern and northeastern New Mexico and in agreement with the $\delta^{18}O$ estimated elevations of 1200–1700 m (3900–5600 ft) above mean sea level. Along the flow path, as salinity increases, molar ratios of Na/Cl and Ca/SO_4 approach 1 as in halite and anhydrite/gypsum (Figures 4 and 5), indicating either dissolution of evaporite minerals or mixture with formation water as a major source of salinity. Conventional thinking is that abundant anhydrite and halite in Ochoan units below the Dockum (Dutton and Simpkins, 1986) are a likely source of these minerals (Figure 2). However, the $^{87}Sr/^{86}Sr$ ratio of the high-salinity group I Dockum aquifers waters does not match that of the evaporite minerals (Figure 8), and the vast majority of group I waters are isotopically distinct ($\delta^{18}O$ and δ^2H) from formation water within the ECS including the Ochoan evaporites (Figure 7; Figure A4 in the Appendix). Thus, the high-salinity group I waters in the Dockum in the study area are not likely waters that have migrated up from the ECS. This interpretation is supported by geologic underpressuring in ECS reservoirs within the Midland Basin and a conceptual groundwater model for the basin of net downward flow through the evaporites since at least the start of the Cenozoic (Engle et al., 2016). However, samples with the highest salinities and with Na/Cl and Ca/SO_4 molar ratios near 1 overlap with regions of established Permian evaporite dissolution (Hovorka, 1998). One mechanism that may explain these incongruent lines of evidence is flow of low-salinity water from the Dockum into the very top of the Permian salt beds, near-horizontal flow across the basin, followed by topographic-driven flow back into the Dockum in areas where structures produce locally upward flow, as suggested by Hovorka (1998) and Barnaby et al. (2004). In this case, the samples representing ECS waters may be hydrologically isolated from the Dockum waters that interact with the evaporites shallower in the Permian sequence. Alternatively, some of the salinity in group I Dockum Aquifer waters may be because of dissolution of evaporite minerals found within the Dockum and overlying aquifers (Dutton and Simpkins, 1986); previous authors have noted anhydrite and halite hoppers in the Dockum (McGowen et al., 1979). Gypsum is also found in abundance in some of the overlying units such as the Edwards–Trinity (Nance, 2004) and could also explain

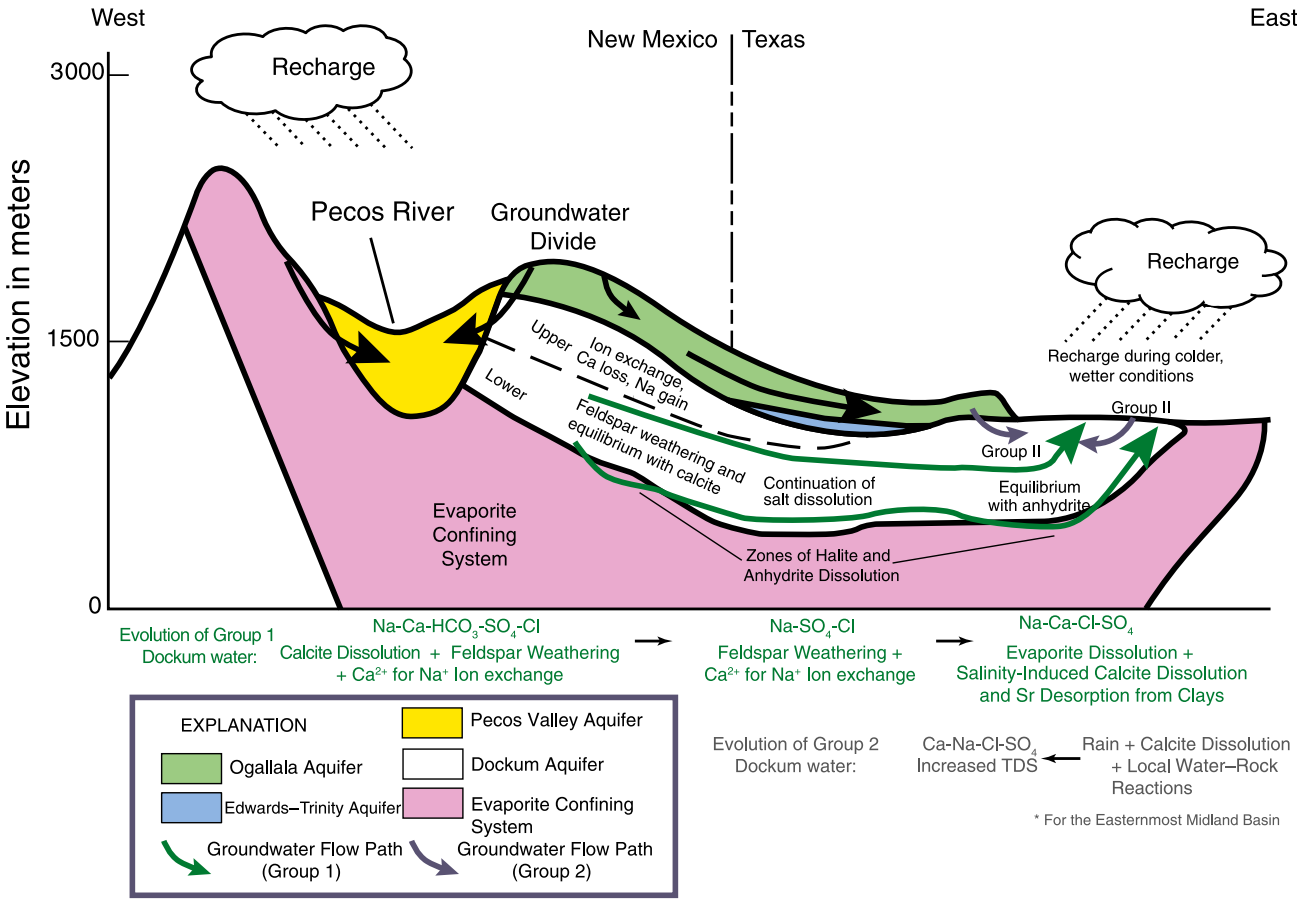

Figure 9. Conceptual model showing flow paths and geochemical reactions controlling the composition of Dockum Aquifer groundwater in the study area. Background cross section modified from Dutton and Simpkins (1986) and Bradley and Kalaswad (2003). TDS = total dissolved solids.

why the lower-TDS group II Dockum waters tend to approach anhydrite saturation (Figure A2 in the Appendix) and why $\delta^{34}S$ values in some of the higher-salinity Dockum samples overlap with early-Cretaceous seawater (Figure A5 in the Appendix). As discussed in the Sequential Extraction of Dockum Rock Samples section, the release of Sr from carbonate and clay minerals within the Dockum Aquifer (because of the influx of high-salinity water in areas of evaporite dissolution) appears to control $^{87}Sr/^{86}Sr$ data from group I Dockum aquifer samples. On the eastern edge of the study area, where the Dockum crops out or is only covered by thin sheets of sedimentary rocks, the presence of saline group I waters present a potential source of shallow groundwater salinity (cf. Figure 6 and Figure A3 in the Appendix). Similar hydrologic conditions exist just southeast of this study area (Figure 1), where Dutton et al. (1989) identified upward flow of subsurface brines from Permian units.

The composition of group II Dockum groundwater in the Midland Basin is primarily controlled by local inflow from overlying aquifers linked with water–rock interactions with carbonates and sandstones (Nance, 2004; Bumgarner et al., 2012) and, particularly in the northeast part of the study area, is influenced by recent local recharge (Ewing et al., 2008; Deeds et al., 2015). For instance, previous scientists have suggested that the Group II water near the southwest corner of the study area represents recharge from regional groundwater flow from far-west Texas and/or southeast New Mexico and runoff from the Barilla, Davis, and Glass Mountains into overlying aquifers (Bumgarner et al., 2012). Elevation estimates from the $\delta^{18}O$ results (1700–2400 m [5600–7900 ft] above mean sea level) for these samples correspond to higher elevation ranges in these regions. Both Na/Cl and Ca/SO_4 ratios show no clear trend with salinity for the group II water samples (Figures 4 and 5), suggesting that evaporite dissolution is not an important

solute source for these waters. Generally, the hydraulic head data for wells screened in the Dockum Aquifer relative to overlying freshwater and brackish aquifers suggest downward flow into the Dockum is likely (Bradley and Kalaswad, 2003) and therefore is a potential source for the relatively dilute brackish group II Dockum groundwater in the southwest Midland Basin. In addition, the group II solutions are in equilibrium with respect to dolomite, quartz, and calcite and are slightly undersaturated with respect to gypsum (Figure A2 in the Appendix); these findings are similar to those of Nance's (2004) data for the overlying Edwards–Trinity aquifer. The Dockum groundwater samples analyzed for δ^2H and $\delta^{18}O$ (Figure 7) share isotopic and Cl concentration similarities with overlying Edwards–Trinity groundwater; this relationship suggests mixing between aquifers or similar recharge sites (Figure A4 in the Appendix). However, a few group II Dockum groundwaters contain less Cl, are moderately depleted in ^{18}O (Figure 7) relative to Edwards–Trinity data, and are located near the edge of the Midland Basin and on the Ozona Arch (Figure 6). This geochemical signature may represent a different recharge site for these group II groundwater samples, relative to data from Bumgarner et al. (2012). These findings suggest that the relatively low–salinity group II waters (almost entirely <5 g TDS/L) are likely locally recharged waters that have developed a broad range in chemical composition based on the mineralogy of the Dockum and overlying aquifers found locally (Figure 10). Although no age-dating techniques were applied, it is assumed that these waters are younger than the group I waters in the study area.

SUITABILITY OF DOCKUM AQUIFER GROUNDWATER FOR USE IN HYDRAULIC FRACTURING FLUID

Brackish groundwaters, analogous to those found in the Dockum Aquifer, can be used as alternative water resources to help meet the growing energy demands in the United States. In the Midland Basin, the greatest water-intensive demands related to hydrocarbon production are those of slick-water and cross-linked gel hydraulic fracturing systems (Scanlon et al., 2017). Gel-based fracturing fluids are high-viscosity fluids that can entrain large quantities of proppant (e.g., sand, ceramic beads, or ceramic-coated sand) to keep fractures open after hydraulic fracture stimulation (King, 2012). By comparison, slick-water fluids are low-viscosity fluids, which typically contain friction reducers among other additives and carry a lower proppant load, and have been used very effectively in shales. Within the Permian Basin, horizontally drilled wells with multistage hydraulic fracturing within individual shale plays (e.g., Wolfcamp, "Cline," Avalon, and Bone Springs shales) have relied heavily on slick-water or hybrid (most stages fractured by slick water with gel used in the final stage[s]) fracture stimulation, whereas vertical wells with perforations in multiple units (e.g., Wolfberry play) have relied more on gel-based fluids. Both types of hydraulic fracturing fluids have potential to use brackish water, but each has specific water quality requirements. Oil and gas operators in the study area provided those criteria for both types of fracturing fluids (Table 4).

Generally, Dockum Aquifer groundwater meets these requirements for use in either slick-water or gel fracturing fluids. Comparison of spatial concentration data for Dockum Aquifer groundwater (Reyes, 2014) with the chemical thresholds (Table 4) can be used to identify areas most suitable for hydraulic fracturing fluid use. Unlike for agricultural use (Dutton and Simpkins, 1986), the salinity of Dockum Aquifer groundwater is not a limiting factor in its use for hydraulic fracturing; only a small percentage (<7%) of Dockum Aquifer groundwater samples have TDS values above the 40 g/L threshold for slick-water fracturing fluids. Other than these very few saline samples, no other geochemical criteria identified limitations for use of Dockum Aquifer groundwater in slick-water fracturing fluid. However, some regions in the study area exhibited SO_4 concentrations exceeding some of the criteria, limiting its use for gel-based fluids. The areas, which are primarily impacted by elevated SO_4 as denoted in Figure 10, are present in the northern and southeastern edges of the Midland Basin. Moreover, the Dockum Aquifer is generally deeper in the northwest part of the basin, which increases the cost to drill production wells and to pump water from those depths. In the part of the basin where the Dockum crops out (Figure 3), chemistry of Dockum Aquifer groundwater is highly variable, so potential for spatially, and possibly temporally, variable water quality would need to be anticipated. In an attempt to understand the potential for scale formation during hydraulic fracturing when the injected water reacts with formation water or to mimic instances of mixing recycled produced water with brackish groundwater, geochemical modeling was performed to examine relative mixtures of Dockum end members (low-salinity group II water, high-salinity group II

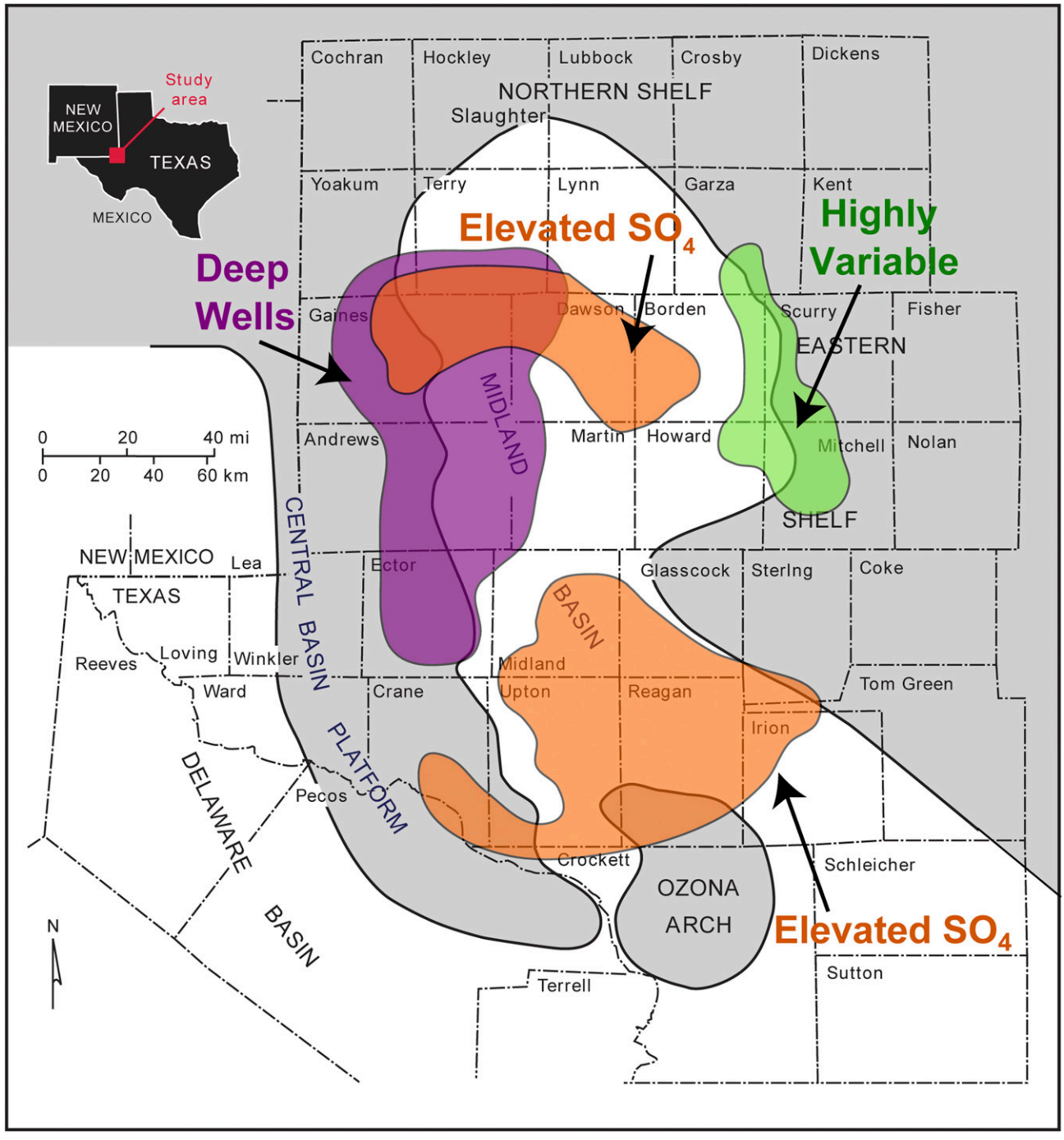

Figure 10. Map showing potential incompatibility or limitations for use of Dockum Aquifer water in hydraulic fracturing fluids. Base map modified from Dutton et al. (2005).

water, low-salinity group I water, and high-salinity group I water) and formation brine (using average compositional data from the unconventional Wolfcamp, Strawn, and Spraberry reservoirs using data from Blondes et al., 2016b). Preliminary modeling results indicate that mixtures of Dockum groundwater end members (high- and low-TDS end members for group I, and high- and low-TDS end members for group II) and 25%–75% of contributions from formation brines are typically supersaturated or saturated with respect to carbonate minerals (calcite and aragonite [$CaCO_3$]) and celestite ($SrSO_4$) but are undersaturated with respect to barite ($BaSO_4$) (Figure A6 in the

Table 4. Acceptable Ranges of Chemical Parameters for Water Used in Cross-Linked Gel Versus Slick-Water Hydraulic Fracturing Fluids.

Hydraulic Fracture System	Cross-Linked Gel Fluid	Slick-Water Fluid
pH	6.0–8.0	>5
Ca + Mg (mg/L)	<2000	–
Fe (mg/L)	<20	–
SO_4 (mg/L)	200–1000	–
Cl (mg/L)	<40,000	–
HCO_3 (mg/L)	<1000	–
B (mg/L)	<10	–
Multivalent ions (mg/L)	–	<5000
TDS (g/L)	–	<40
Reducing agent (mg/L)	<25	–

Information obtained and compiled from multiple oil and gas producers within the study area. Reducing agents include compounds such as hydrogen sulfide and ferrous iron.

Abbreviation: – = no requirement.

Appendix). Barite undersaturation is important given its extremely low-solubility product, difficulty in removing it from pipes and the reservoir, and its potential to accumulate radium. Data were lacking to determine silica saturation in this exercise. Overall, mineral precipitation during the injection of the Dockum should be manageable, especially if scale inhibitors are used. These calculations are based on average compositions to serve as an example and need to be recalculated for specific cases.

Although the total volume of Dockum Aquifer water within the study area that meets requirements for use as either slick-water or cross-linked gel fracturing fluid is unknown, the Dockum Aquifer in the study area contains more than 1.0×10^{11} m^3 (~2.7×10^{13} gal) of water (using data from Bradley and Kalaswad, 2003), of which approximately 25% of that is greater than 10 g/L TDS. Compared to a typical value of 18,900 m^3 (5×10^6 gal) of water needed for hydraulic fracturing per well within the study area (Scanlon et al., 2017), a large enough volume of water is present in the Dockum Aquifer to accommodate oil and gas operations for decades or longer. Concern is given to the large range in transmissivity values (2 to 990 m^2/day [20 to 11,000 ft^2/day]) reported for the Dockum (Reyes, 2014), suggesting some risk for low flow in drilled wells. However, both previous reports (Bradley and Kalaswad, 2003) and informal discussion with drillers have noted higher permeability in basal conglomerates and the Santa Rosa sandstone within the Dockum aquifer, whose locations can be identified from geophysical well logs. In the southern and eastern parts of the study area, where the Dockum crops out or is in hydraulic communication with overlying aquifers (Nance, 2004), substantial withdrawal from the Dockum Aquifer could produce lower water levels in overlying freshwater aquifers. In the rest of the basin, the lower Dockum is hydrologically isolated and receives little modern recharge (Bradley and Kalaswad, 2003), suggesting that any significant withdrawal is unsustainable but is less likely to impact water levels in overlying freshwater aquifers. Despite these cautions, potential for increased application of brackish water from the Dockum Aquifer in hydraulic fracturing fluids in the Permian Basin is promising.

CONCLUSIONS

This study examines the origin and evolution of groundwaters in the Dockum Aquifer brackish groundwater system overlying the Midland Basin in Texas. We identified two basic types of waters in the Dockum: high-TDS group I waters that show increasing salinity along the flow path because of increasing dissolution of evaporites and group II waters that are locally sourced, commonly from overlying aquifers, showing a much more variable composition. Findings show that in this case, the origin and controls in the Dockum include conventional water–rock interactions (i.e., quartz and calcite buffering, incongruent feldspar weathering, and ion exchange), which are also typical reactions in shallow groundwater systems. However, the potential for upward flow of basinal brines (not occurring in this case but is known to occur in other basins), dissolution of evaporate minerals, high-salinity–induced calcite dissolution and cation desorption from clays, and variations in climate and/or topography provide added complexity less common in shallow, freshwater aquifer systems.

Comparison of water quality requirements for slick-water and cross-linked gel fracturing fluids suggest that the majority of Dockum Aquifer water within the study area can be used with little to no treatment, barring some regions of high SO_4 that might prevent problems for the latter. Potentially, dilution or mixing with SO_4-poor produced waters or application of engineering methods (nanofiltration or sulfate selective ion exchange) may solve this issue for areas producing SO_4-elevated Dockum groundwater, depending on the specific requirements and costs. Despite this scenario, there are still significant barriers to overcome in the

more extensive application of brackish groundwaters for hydraulic fracturing within the Permian Basin and elsewhere. In some cases, lease owners dictate that to lease their mineral rights, oil and gas operators are required to purchase water for hydraulic fracturing from them. Anecdotally, purchased water is primarily from relatively shallow aquifers that might be better used for other purposes. Moreover, the substantial range and variations in compounds used in hydraulic fracturing (King, 2012) prevent testing for compatibility between these compounds and the broad range in chemistry found even within a single brackish water source. Such problems have previously been overcome by use of freshwater, which has few solutes likely to produce deleterious reactions in the fracturing fluid. Finally, although a combination of drought conditions, highly constrained water resources, and environmental responsibility on the part of oil–gas operators allowed for drilling and characterization of brackish groundwaters in the study area, substantially less information on brackish groundwater systems is available in other oil-producing basins. Thus, significant work still remains to expand application and use of brackish groundwater to reduce freshwater use during hydrocarbon exploration and development.

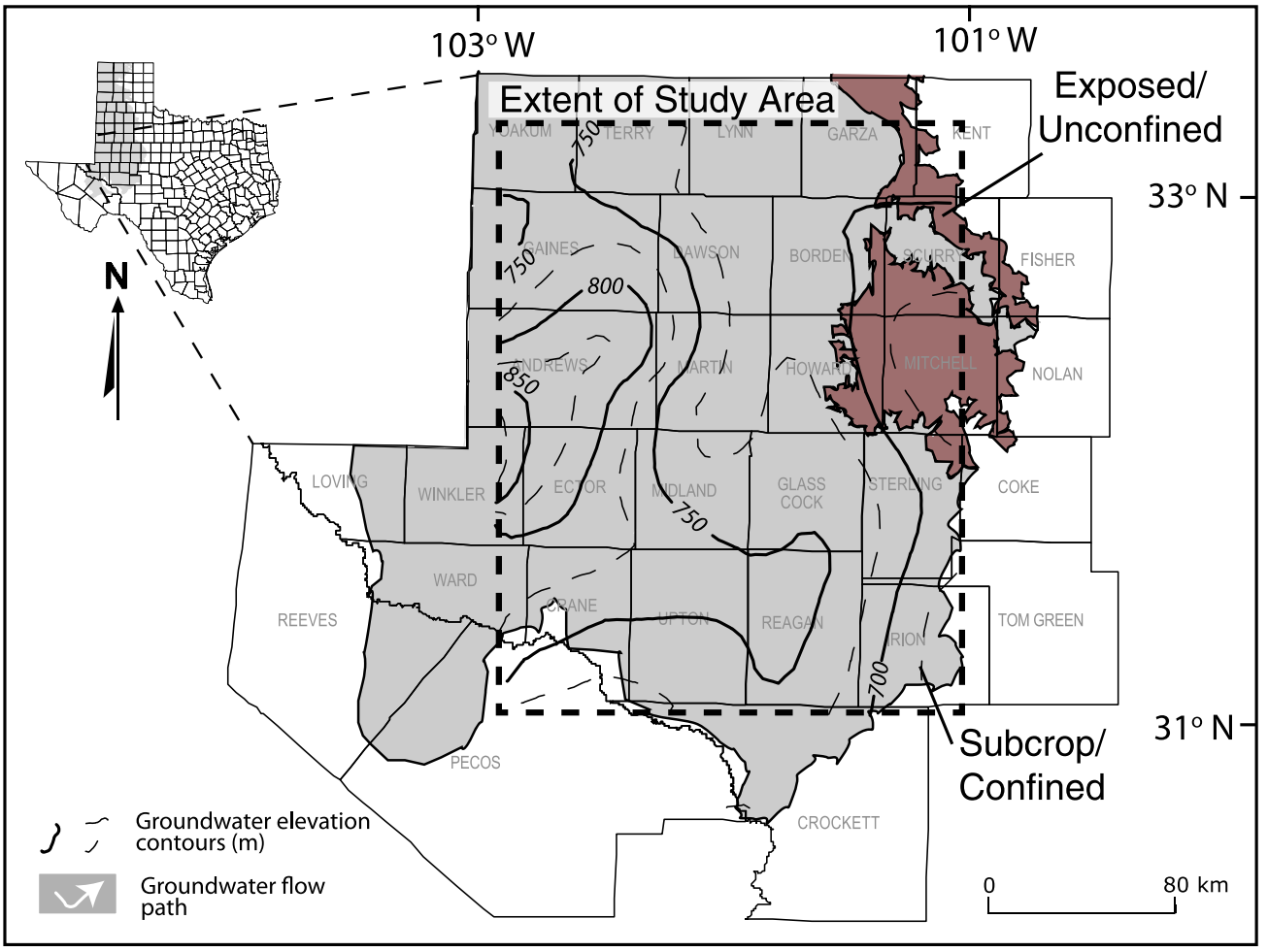

Figure A1. Map showing contours of hydraulic head across the study based on data from the Texas Water Development Board. Base map modified from Bradley and Kalaswad (2003).

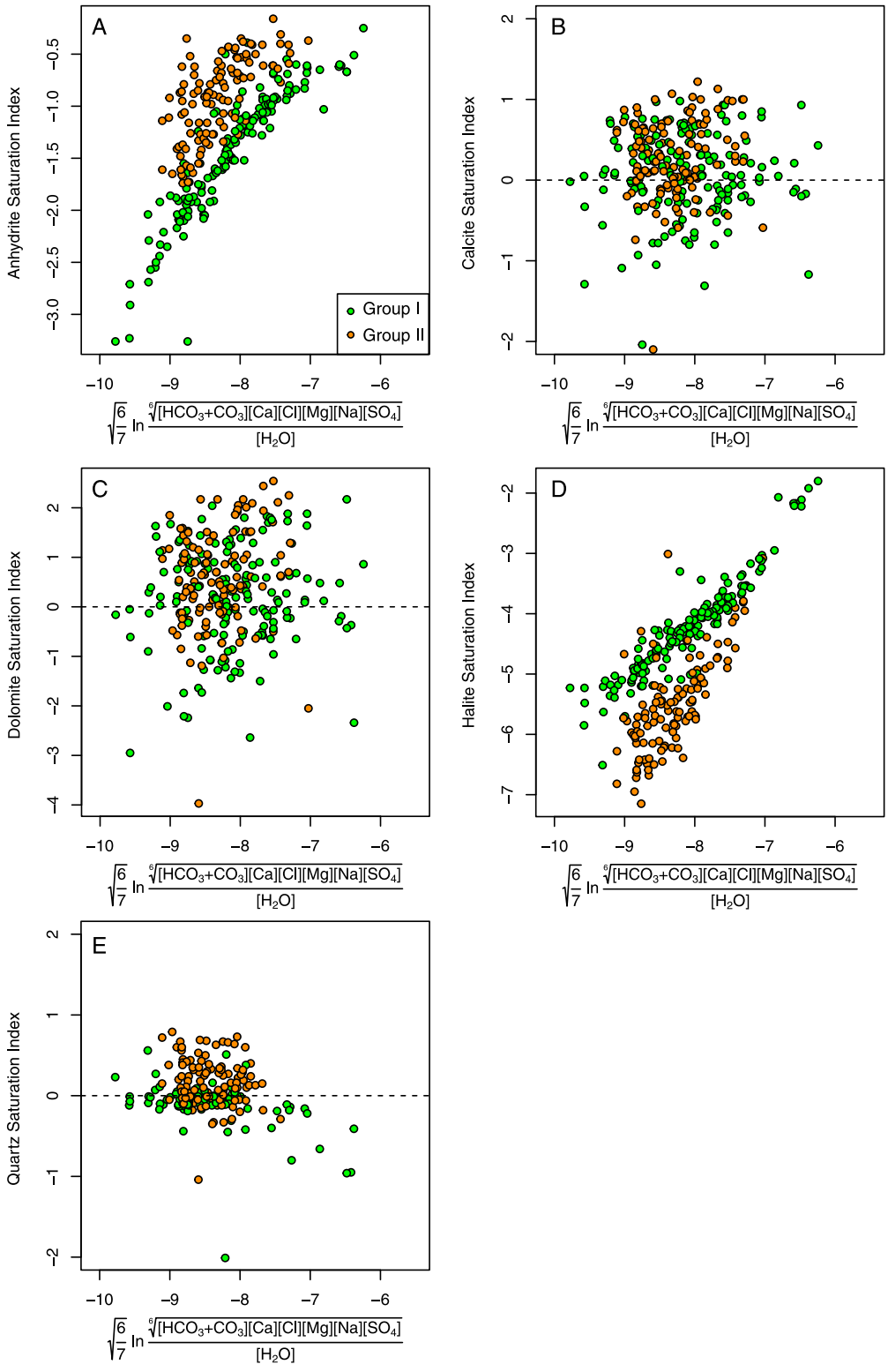

Figure A2. Saturation index of anhydrite (A), calcite (B), dolomite (C), halite (D), and quartz (E) as a function of the isometric log-ratio proxy for salinity in Dockum Aquifer groundwater.

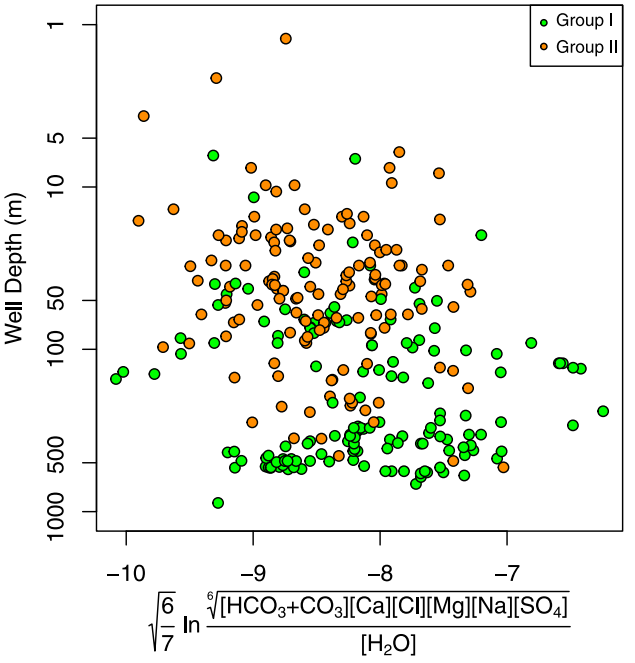

Figure A3. Relationship between well depth (log scale) and the isometric log-ratio proxy for salinity in Dockum Aquifer waters.

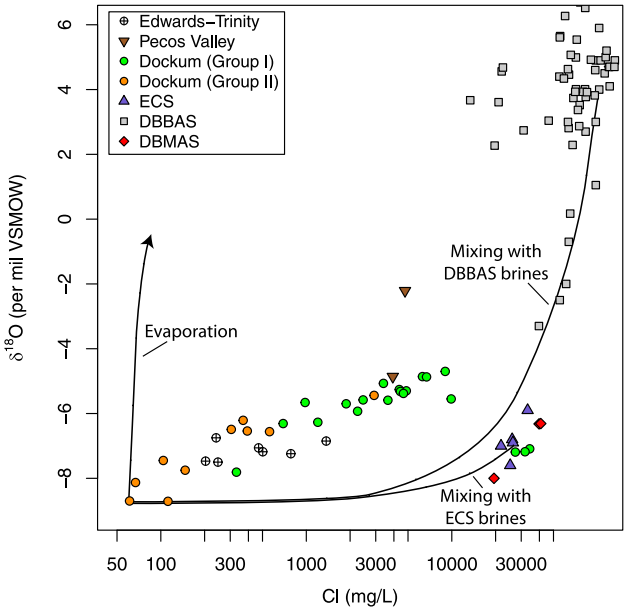

Figure A4. Bivariate plot of $\delta^{18}O$ versus Cl concentration data for groundwater samples collected within the Midland Basin. Increasing evaporation trajectory was calculated using a Rayleigh distillation model at 25°C (model stops at 30% evaporated fraction). Deep Basin Brine Aquifer System (DBBAS)–Dockum and Evaporite Confining System (ECS)–Dockum mixture trajectories are calculated with a two-component mixing model between a dilute Dockum end member and a median value for the brine end member. VSMOW = Vienna standard mean ocean water.

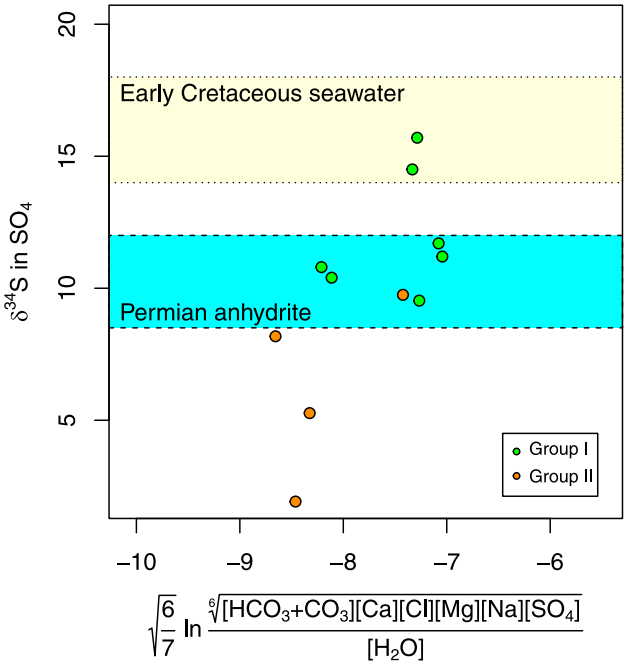

Figure A5. Bivariate plot of $\delta^{34}S$ in SO_4 versus the isometric log-ratio salinity proxy Dockum Aquifer groundwater samples. Ranges of $\delta^{34}S$ in mineral sources taken from Claypool et al. (1980) and Hovorka et al. (1993).

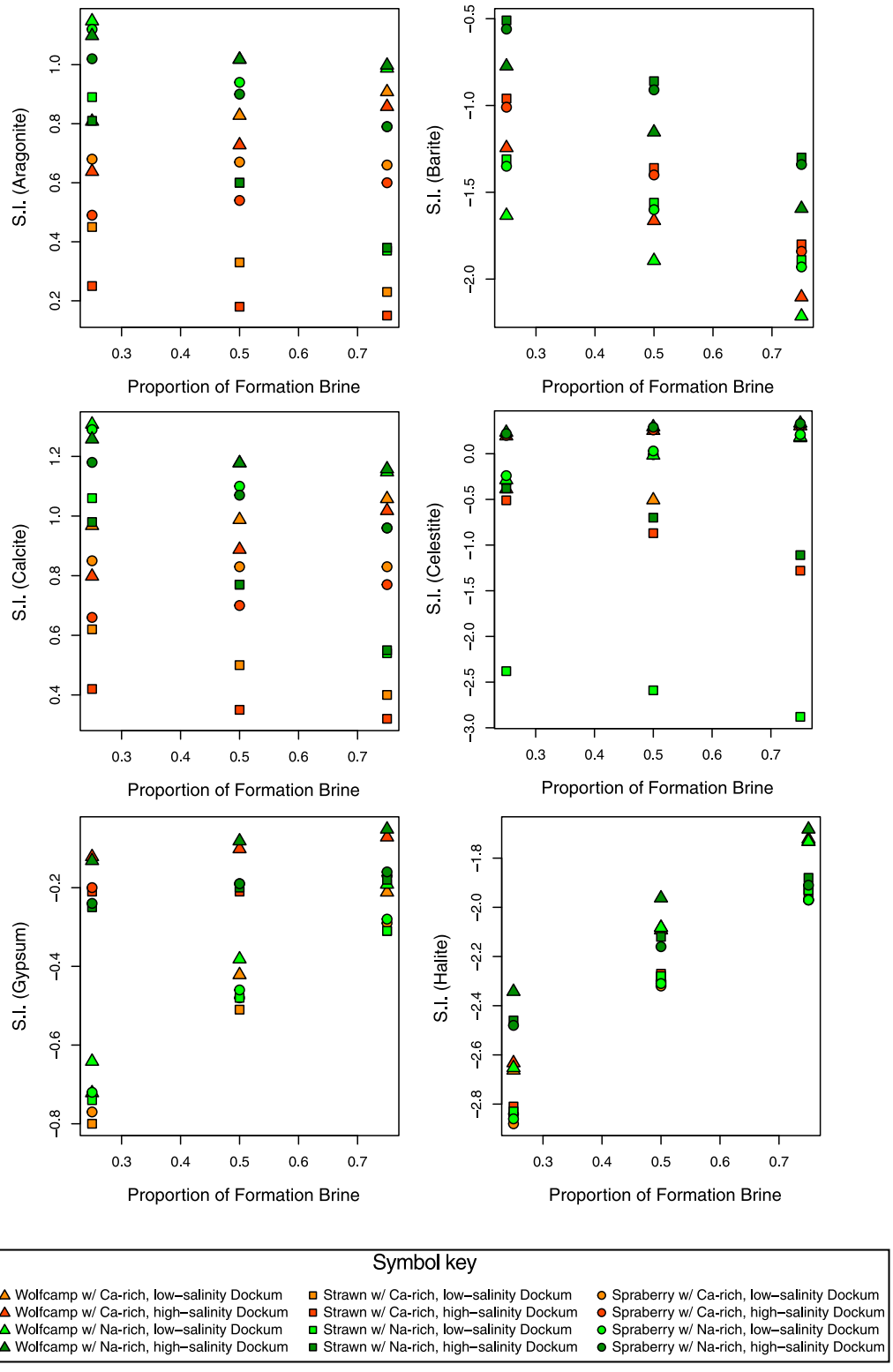

Figure A6. Calculated mineral saturation indices (S.I.) for mixtures between different Dockum end members (see text) and produced waters from the Wolfcamp, Strawn, and Spraberry reservoirs for aragonite, barite, calcite, celestite, gypsum, and halite.

Table A1. Sampling, Location, Field Parameter, and Chemical Information for New Samples Presented in This Effort

Sample ID	Aquifer	Sampling Event	Latitude, °	Longitude, °	Well Depth, m (ft)	Temperature, °C	Sp. Cond., mS/cm	pH	Eh, mV	DO, mg/L	TDS, mg/L	B, mg/L	Ba, mg/L	Br, mg/L
UAS-1	Edwards–Trinity	September, 2012	31.52	−101.98	457 (1500)	22.60	3.075	6.85	−72.1	0.24	1770	1.16	0.006	0.13
UAS-2	Edwards–Trinity	September, 2012	31.51	−101.98		21.31	1.908	7.35	98.2	12.86	1680	1.13	0.007	0.13
UAS-3	Edwards–Trinity	September, 2012	31.16	−101.77	481 (1580)		11.270	7.80			2620	0.81	0.006	1.68
UAS-4	Edwards–Trinity	September, 2012	31.30	−101.37			16.500	8.20			1380	0.5	0.022	1.17
UAS-5	Edwards–Trinity	September, 2012	31.23	−101.22		21.16	2.191	7.21	88.7	5.14	749	0.09	0.017	0.61
UAS-6	Edwards–Trinity	September, 2012	31.50	−101.05			28.610	7.98			1660	0.85	0.007	0.05
Dockum-1	Dockum	July, 2013	32.41	−102.25	524 (1720)	22.17	8.280	7.79	−217.2	0.29	4480		0.104	3.38
Dockum-2	Dockum	July, 2013	32.41	−102.17	512 (1680)	26.39	4.882	7.84	−159.9	0.42	3160		0.078	3.35
Dockum-3	Dockum	September, 2012	32.28	−102.09	671 (2200)	22.28	2.148	7.09	50.2	6.40	4560	0.69	0.018	3.71
Dockum-4	Dockum	July, 2013	31.48	−102.02	354 (1160)	20.84	2.173	7.21	−13.0	4.98	1650		0.039	0.33
Dockum-5	Dockum	September, 2012	31.44	−102.01	419 (1375)	25.44	15.330	7.69	−220.2	0.02	10,500	0.65	0.044	7.18
Dockum-6	Dockum	July, 2013	32.07	−102.00		26.39	10.030	7.45	−141.1	0.22	6470		0.099	3.00
Dockum-7	Dockum	September, 2012	31.52	−101.99	471 (1545)	23.07	2.669	7.07	136.5	0.83	13,700	0.67	0.045	8.65
Dockum-8	Dockum	September, 2012	31.79	−101.96	390 (1280)	20.56	2.305	7.09	−62.0	3.45	10,800	0.71	0.047	9.59
Dockum-9	Dockum	September, 2012	31.85	−101.95	449 (1475)	21.00	2.130	7.21	24.0	1.00	10,800	0.61	0.04	10.0
Dockum-10	Dockum	September, 2012	31.46	−101.94	518 (1700)	21.77	1.221	7.38	−16.9	1.93	1910	0.35	0.023	0.11
Dockum-11	Dockum	September, 2012	31.46	−101.94	488 (1600)	24.95	21.190	7.52	−175.0	0.14	7640	0.36	0.024	6.25
Dockum-12	Dockum	July, 2013	31.85	−101.93	335 (1100)	25.17	17.500	7.38	−111.1	0.51	11,400		0.253	6.01
Dockum-13	Dockum	September, 2012	32.26	−101.91	299 (980)		6.200	6.98			4820	0.21	0.009	6.39
Dockum-14	Dockum	September, 2013	31.93	−101.87	610 (2000)	25.58	14.180	7.41	19.1	0.54	9610	0.26	0.005	20.7
Dockum-15	Dockum	July, 2013	31.93	−101.82	360 (1180)	25.21	14.570	7.23	−135.7	0.42	9550		0.224	4.87
Dockum-16	Dockum	September, 2012	31.17	−101.80	355 (1165)	21.20	1.870	7.36	84.9	1.45	1970	0.65	0.007	1.03
Dockum-17	Dockum	September, 2012	31.21	−101.78	454 (1490)		21.300	7.95			2370	1.11	0.007	1.53
Dockum-18	Dockum	July, 2013	31.27	−101.78		20.39	2.651	6.52	50.5	2.54	2310		0.041	0.53
Dockum-19	Dockum	September, 2012	31.16	−101.77	481 (1580)	30.45	8.366	7.92	−302.8		14,700	0.52	0.035	10.5
Dockum-20	Dockum	September, 2012	32.45	−101.77	360 (1180)		8.700	7.77			6890	0.45	0.011	15.0
Dockum-21	Dockum	September, 2013	31.15	−101.25		20.92	2.695	7.12	−14.0	0.68	1960	0.99	0.011	3.16
Dockum-22	Dockum	September, 2013	32.61	−101.25		21.84	32.860	7.21	−25.1	0.24	21,900	0.6	0.012	20.0
Dockum-23	Dockum	September, 2013	32.80	−101.20		22.29	93.040	5.87	18.2	0.90	38,900	1.60	0.032	40.0
Dockum-24	Dockum	September, 2013	31.18	−101.17	223 (730)	20.77	3.600	7.00	−84.3	0.59	2400	0.63	0.012	2.91
Dockum-25	Dockum	September, 2013	31.22	−101.11	238 (780)	20.91	3.669	7.37	−45.6	1.13	2540	0.55	0.01	4.28
Dockum-26	Dockum	September, 2013	31.28	−101.05	195 (640)	22.10	2.945	7.03	−96.0	1.14	2090	0.42	0.013	2.89
Dockum-27	Dockum	September, 2013	32.59	−101.05	132 (435)	21.23	83.520	6.75	0.1	0.20	55,700	1.52	0.031	37.1
Dockum-28	Dockum	September, 2012	31.50	−101.04	426 (1400)	25.82	15.460	7.73	−226.3	0.02	18,600	0.71	0.047	10.5
Dockum-29	Dockum	September, 2013	32.58	−101.04	130 (425)	21.25	83.400	6.78	14.3	0.29	38,900	1.50	0.031	34.4

Ca, mg/L	Cl, mg/L	Fe, mg/L	K, mg/L	Li, mg/L	Mg, mg/L	Na, mg/L	NO_3, mg/L	Si, mg/L	Sr, mg/L	SO_4, mg/L	Alkalinity (as $CaCO_3$), mg/L	DOC, mg/L	$^{87}Sr/^{86}Sr$	$\delta^{18}O_{water}$ (concentration basis), ‰	$\delta^{2}H_{water}$ (concentration basis), ‰	$\delta^{34}S_{sulfate}$, ‰
247	66		19.6	0.3	98	163	20.5	4.91	4.9	974	181	0.442	0.70874	−8.89	−63.52	8.24
329	62		17.9	0.33	102	134	27.3	5.27	6.49	1070	162	0.195	0.70867	−8.83	−61.57	8.16
409	169		10.5	0.23	203	192	3.0	7.26	7.26	1520	294	0.917	0.70848	−8.32	−57.96	2.35
138	222		9.35	0.14	72.1	190	10.1	6.92	11.3	507	228	0.302	0.70788	−6.27	−43.42	10.0
136	102		4.82	0.09	62.5	83	5.6	8.63	14.8	310	226	0.378	0.70777	−5.96	−40.19	9.07
238	42		15.6	0.23	102	135	48.9	4.91	4.03	921	176	0.341	0.70875	−8.21	−57.63	7.22
57	1880	1.88	21.6	2.17	25.5	1580	0.9	2.73	2.16	1230	289	0.819	0.70859	−5.70	−40.78	
13	693	0.18	12.5	1.33	4.1	993	0.5	4.46	0.238	919	578	0.819	0.70873	−6.31	−43.52	
50	1200		21.0	0.41	24.7	1450	1.5	5.78	0.86	1360	555	0.149	0.70872	−6.27	−45.65	10.4
171	61	0.10	25.4	0.71	84.4	229	7.9	3.58	3.57	926	234	0.819	0.70880	−8.70	−61.19	
346	4870		82.1	1.71	211	3470	3.4	0.96	7.98	1780	176	0.655	0.70944	−5.30	−38.45	9.53
88	2250	0.69	33.4	2.8	28.3	2000	1.1	4.37	1.72	1710	370	0.819	0.70904	−5.93	−42.82	
422	6290		112	2.18	206	4670	8.6	3.78	15.9	2270	221	0.143	0.70968	−4.86	−34.52	11.7
277	4360		55.1	1.67	137	3720	3.2	3.64	11.9	2430	226	0.169	0.70990	−5.26	−37.29	15.7
258	4430		56.3	1.51	141	3640	3.5	4.00	10.7	2460	174	0.231	0.70977	−5.32	−38.09	14.5
326	67		11.4	0.29	96.3	138	36	4.50	5.65	1030	161	0.234		−8.13	−57.20	8.18
327	2920		65.2	1.31	164	2330	2.8	3.08	8.9	1860	215	0.048	0.70934	−5.44	−39.20	9.75
272	4650	4.14	62.2	4.43	98.9	3450	2.0	3.94	7.77	2560	294	0.819	0.70961	−5.38	−39.74	
83	981	0.06	12.5	3.8	30.4	1350	2.3	3.26	3.09	1190	286		0.70888	−5.66	−40.52	
140	3390	0.44	27.1	5.48	62.7	2950	7.9	3.66	4.92	2380	307	0.305	0.70940	−5.07	−38.34	
187	3640	0.10	46.4	3.67	66.3	2950	1.6	3.89	5.25	2410	332	0.819	0.70943	−5.59	−39.98	
246	104		8.83	0.17	164	150	1.1	5.94	4.86	973	280	0.603	0.70846	−7.45	−51.34	1.92
326	147		11.4	0.22	165	185	1.8	4.8	5.45	1260	225	0.693	0.70855	−7.75	−54.63	5.27
247	112	0.02	25.3	0.72	120	254	15.9	4.26	5.17	1190	217	0.819	0.70863	−8.71	−60.54	
573	6700		0.46	1.9	0.1	4590	2.6	0.07	13.3	2560	185	0.214	0.70920	−4.87	−34.49	10.8
59	2460	0.04	8.97	4.49	27	2210	6.3	3.52	2.26	1440	467		0.70854	−5.58	−40.94	
119	305	2.06	15.0	0.94	112	352	1.6	3.75	5.17	717	299	0.305	0.70824	−6.49	−45.92	
521	9900	2.14	51.3	14.2	167	6900	19.6	1.62	11.4	3300	277	0.305	0.70891	−5.55	−39.06	
1920	34,300	29.1	187	50.4	608	21,700	44.9	2.23	54.3	2630	62.9	1.42	0.70951	−7.09	−49.97	
176	393	6.28	20.3	1.17	127	459	22.1	3.76	6.81	628	310	0.305	0.70809	−6.54	−46.47	
193	559	1.6	16.5	1.29	133	464	2.0	4.12	4.76	863	292	0.305	0.70838	−6.56	−44.86	
165	368	2.92	14.5	1.02	101	356	4.2	3.74	5.71	484	260	0.305	0.70807	−6.21	−43.31	
1400	31,900	2.99	66.3	33	433	18,000	46.3	0.65	41	2590	106	0.305	0.70944	−7.18	−50.19	
616	9010		146	2.8	333	6450	9.7	3.52	17	2610	52.1	0.325	0.70964	−4.70	−34.29	11.2
1410	27,300	3.3	136	39.9	436	18,000	43.1	0.64	41.3	2200	106	0.305	0.70946	−7.19	−49.42	

Blank cells indicate either data were not available (i.e., well depth), impacted by problems with field sensors (i.e., Eh and pH), failed quality assurance and quality control checks (i.e., compositional data), were lacking volume (i.e., dissolved organic carbon [DOC] and $^{87}Sr/^{86}Sr$), or were not analyzed ($\delta^{34}S$).
Abbreviation: Sp. Cond. = specific conductance; TDS = total dissolved solids.

Table A2. Concentration of Elements Found in Sequential Extraction Solutions of Dockum Rock Samples

Extraction Solution	Ba	Ca	Fe	K	Mg	Si	Sr
			Upper Dockum (Trujillo): Outcrop Sample				
DI leach	<0.0006	<0.06	<0.006	0.064	<0.0006	0.0032	0.00032
4 M acetic acid leach	0.0044	29.8	<0.03	0.099	0.105	<0.15	0.0155
1 M HCl leach	0.0076	18.5	0.030	0.049	0.077	0.0071	0.0095
			Lower Dockum (Santa Rosa): Cuttings Sample				
DI leach	<0.0006	0.018	<0.005	0.083	0.0072	0.0043	0.00079
4 M acetic acid leach	0.0046	15.1	0.017	0.060	0.32	0.050	0.0327
1 M HCl leach	0.016	5.73	0.13	0.12	0.24	0.023	0.0157

Units are milligrams of element per gram of rock sample.
Abbreviation: DI = deionized.

REFERENCES CITED

Barnaby, R. J., G. C. Oetting, and G. Gao, 2004, Strontium isotopic signatures of oil-field waters: Applications for reservoir characterization: AAPG Bulletin, v. 88, no. 12, p. 1677–1704, doi:10.1306/07130404002.

Bassett, R. L., and M. E. Bentley, 1982, Geochemistry and hydrodynamics of deep formation brines in the Palo Duro and Dalhart basins, Texas, U.S.A.: Journal of Hydrology, v. 59, no. 3–4, p. 331–372, doi:10.1016/0022-1694(82)90095-6.

Bein, A., and A. R. Dutton, 1993, Origin, distribution, and movement of brine in the Permian Basin (U.S.A.): A model for displacement of connate brine: Geological Society of America Bulletin, v. 105, no. 6, p. 695–707, doi:10.1130/0016-7606(1993)105<0695:ODAMOB>2.3.CO;2.

Blondes, M. S., M. A. Engle, and N. J. Geboy, 2016a, A practical guide to the use of major elements, trace elements, and isotopes in compositional data analysis: Applications for deep formation brine geochemistry, *in* J. A. Martín-Fernández and S. Thió-Henestrosa, eds., Compositional data analysis: Springer Proceedings in Mathematics & Statistics 187, p. 13–29, doi:10.1007/978-3-319-44811-4_2.

Blondes, M. S., K. D. Gans, E. L. Rowan, J. J. Thordsen, M. E. Reidy, M. A. Engle, Y. K. Kharaka, and B. Thomas, 2016b, US Geological Survey National Produced Waters Geochemical Database v2.2 (Provisional), accessed October 11, 2016, https://eerscmap.usgs.gov/pwapp/.

Bradley, R. G., and S. Kalaswad, 2001, The Dockum Aquifer in West Texas, *in* R. E. Mace, W. F. Mullican III, and E. S. Angle, eds., Aquifers of West Texas: Austin, Texas, Texas Water Development Board, p. 167–174.

Bradley, R. G., and S. Kalaswad, 2003, The groundwater resources of the Dockum Aquifer in Texas: Austin, Texas, Texas Water Development Board Report 359, 73 p.

Buccianti, A., and V. Pawlowsky-Glahn, 2005, New perspectives on water chemistry and compositional data analysis: Mathematical Geology, v. 37, no. 7, p. 703–727, doi:10.1007/s11004-005-7376-6.

Bumgarner, J. R., G. P. Stanton, A. P. Teeple, J. V. Thomas, N. A. Houston, J. D. Payne, and M. Musgrove, 2012, A conceptual model of the hydrogeologic framework, geochemistry, and groundwater-flow system of the Edwards-Trinity and related aquifers in the Pecos County Region, Texas: Reston, Virginia, US Geological Survey Scientific Investigations Report 2012–5124, 74 p.

Claypool, G. E., W. T. Holser, I. R. Kaplan, H. Sakai, and I. Zak, 1980, The age curves of sulfur and oxygen isotopes in marine sulfate and their mutual interpretation: Chemical Geology, v. 28, p. 199–260, doi:10.1016/0009-2541(80)90047-9.

Coleman, J. L. Jr., and S. M. Cahan, 2012, Preliminary catalog of the sedimentary basins of the United States: Reston, Virginia, US Geological Survey Open-File Report 2012-1111, 27 p.

Coplen, T. B., and C. Kendall, 2000, Stable hydrogen and oxygen isotope ratios for selected sites of the US Geological Survey's NASQAN and benchmark surface-water networks: Reston, Virginia, US Geological Survey Open-File Report 00-160, 409 p.

Dansgaard, W., 1964, Stable isotopes in precipitation: Tellus. Series A, Dynamic Meterology and Oceanography, v. 16, no. 4, p. 436–468, doi:10.1111/j.2153-3490.1964.tb00181.x.

Deeds, N. E., J. J. Harding, T. L. Jones, A. Singh, INTERA Incorporated, S. Hamlin, R. C. Reedy, et al, 2015, Final conceptual model report for the High Plains Aquifer System Groundwater Availability Model: Austin, Texas, Texas Water Development Board, 590 p.

Dutton, A. R., 1995, Groundwater isotopic evidence for paleorecharge in US High Plains aquifers: Quaternary Research, v. 43, no. 2, p. 221–231, doi:10.1006/qres.1995.1022.

Dutton, A. R., B. C. Richter, and C. W. Kreitler, 1989, Brine discharge and salinization, Concho River Watershed, West Texas: Ground Water, v. 27, no. 3, p. 375–383, doi:10.1111/j.1745-6584.1989.tb00461.x.

Dutton, A. R., and W. W. Simpkins, 1986, Hydrogeochemistry and water resources of the Triassic Lower Dockum Group in the Texas Panhandle and Eastern New Mexico: Austin, Texas, Texas Bureau of Economic Geology Report of Investigations 161, 51 p.

Dutton, A. R., and W. W. Simpkins, 1989, Isotopic evidence for paleohydrologic evolution of ground-water flow paths, southern Great Plains, United States: Geology, v. 17, no. 7, p. 653–656, doi:10.1130/0091-7613(1989)017<0653:IEFPEO>2.3.CO;2.

Dutton, S. P., E. M. Kim, R. F. Broadhead, W. D. Raatz, C. L. Breton, S. C. Ruppel, and C. Kerans, 2005, Play analysis and leading-edge oil-reservoir development methods in the Permian basin: Increased recovery through advanced technologies: AAPG Bulletin, v. 89, no. 5, p. 553–576, doi:10.1306/12070404093.

Egozcue, J. J., and V. Pawlowsky-Glahn, 2005, Groups of parts and their balances in compositional data analysis: Mathematical Geology, v. 37, no. 7, p. 795–828, doi:10.1007/s11004-005-7381-9.

El-Assy, N., A. A. Fattah, R. El-Shinawy, and M. W. A. Essa, 1991, Adsorption–desorption equilibria of some radionuclides in sediment-sea water system: Journal of Radioanalytical and Nuclear Chemistry, v. 152, no. 1, p. 31–35, doi:10.1007/BF02042138.

Engle, M. A., and M. S. Blondes, 2014, Linking compositional data analysis with thermodynamic geochemical modeling: Oilfield brines from the Permian Basin, USA: Journal of Geochemical Exploration, v. 141, p. 61–70, doi:10.1016/j.gexplo.2014.02.025.

Engle, M. A., A. Buccianti, R. A. Olea, and M. S. Blondes, 2017, Merging key concepts in the chemistry of natural waters with compositional data analysis: Updates to basic water quality plots, *in* K. Hron and R. Tolosana-Delgado, eds., 7th International Workshop on Compositional Data Analysis, Addadia San Salvatore, Italy, June 5–9, 2017, p. 47–55.

Engle, M. A., F. R. Reyes, M. S. Varonka, W. H. Orem, L. Ma, A. J. Ianno, T. M. Schell, P. Xu, and K. C. Carroll, 2016, Geochemistry of formation waters from the Wolfcamp and "Cline" shales: Insights into brine origin, reservoir connectivity, and fluid flow in the Permian Basin, USA: Chemical Geology, v. 425, p. 76–92, doi:10.1016/j.chemgeo.2016.01.025.

Engle, M. A., and E. L. Rowan, 2013, Interpretation of Na-Cl-Br systematics in sedimentary basin brines: Comparison of concentration, element ratio, and isometric log-ratio approaches: Mathematical Geosciences, v. 45, no. 1, p. 87–101, doi:10.1007/s11004-012-9436-z.

Ewing, J. E., T. L. Jones, T. Yan, A. M. Vreugdenhil, D. G. Fryar, J. F. Pickens, K. Gordon, et al., 2008, Groundwater availability model for the Dockum Aquifer: Austin, Texas, Texas Water Development Board, 510 p.

Gallegos, T. J., B. A. Varela, S. S. Haines, and M. A. Engle, 2015, Hydraulic fracturing water use variability in the United States and potential environmental implications: Water Resources Research, v. 51, no. 7, p. 5839–5845, doi:10.1002/2015WR017278.

Hovorka, S., 1998, Characterization of bedded salt for storage caverns: A case study from the Midland Basin, Texas: Austin, Texas, The University of Texas at Austin, 101 p.

Hovorka, S. D., L. P. Knauth, R. S. Fisher, and G. Gao, 1993, Marine to nonmarine facies transition in Permian evaporites of the Palo Duro Basin, Texas: Geochemical response: Geological Society of America Bulletin, v. 105, no. 8, p. 1119–1134, doi:10.1130/0016-7606(1993)105<1119:MTNFTI>2.3.CO;2.

Jacobson, A. D., J. D. Blum, and C. P. Chamberlain, 2003, Climatic and tectonic controls on chemical weathering in the New Zealand Southern Alps: Geochimica et Cosmochimica Acta, v. 67, no. 1, p. 29–46, doi:10.1016/S0016-7037(02)01053-0.

King, G. E., 2012, Hydraulic fracturing 101: What every representative, environmentalist, regulator, reporter, investor, university researcher, neighbor, and engineer should know about hydraulic fracturing risk: Journal of Petroleum Technology, v. 64, no. 4, p. 34–42, doi:10.2118/0412-0034-JPT.

Konter, J. G., and L. P. Storm, 2014, High precision $^{87}Sr/^{86}Sr$ measurements by MC-ICP-MS, simultaneously solving for Kr interferences and mass-based fractionation: Chemical Geology, v. 385, p. 26–34, doi:10.1016/j.chemgeo.2014.07.009.

McGowen, J. H., G. E. Granata, and S. J. Seni, 1979, Depositional framework of the lower Dockum Group (Triassic), Texas Panhandle: Austin, Texas, Bureau of Economic Geology, The University of Texas at Austin Report of Investigations No. 97, 60 p.

Nance, H. S., 2004, Hydrochemical variability in the Edwards-Trinity aquifer system, Edwards Plateau, Texas, *in* R. E. Mace, E. S. Angle, and W. F. Mullican III, eds., Aquifers of the Edwards Plateau: Austin, Texas, Texas Water Development Board Report 360, p. 63–90.

Nicot, J.-P., R. C. Reedy, R. A. Costley, and Y. Huang, 2012, Oil & gas water use in Texas: Update to the 2011 mining water use report: Austin, Texas, Texas Bureau of Economic Geology, 95 p.

Nicot, J.-P., and B. R. Scanlon, 2012, Water use for shale-gas production in Texas, U.S.: Environmental Science & Technology, v. 46, no. 6, p. 3580–3586, doi:10.1021/es204602t.

Otero, N., R. Tolosana-Delgado, A. Soler, V. Pawlowsky-Glahn, and A. Canals, 2005, Relative versus absolute statistical analysis of compositions: A comparative study of surface waters of a Mediterranean river: Water Research, v. 39, no. 7, p. 1404–1414, doi:10.1016/j.watres.2005.01.012.

Parkhurst, D. L., and C. Appelo, 1999, User's guide to PHREEQC (version 2)—A computer program for speciation, batch-reaction, one-dimensional transport, and inverse geochemical calculations: Reston, Virginia, US Geological Survey Water-Resources Investigations Report 99-4259, 312 p.

Register, J. K., and D. G. Brookins, 1980, Rb-Sr isochron age of evaporite minerals from the Salado formation (Late Permian), southeastern New Mexico: Isochron: Isochron-West, v. 29, p. 39–42.

Reyes, F. R., 2014, Exploring the hydrogeologic controls on brackish water and its suitability for use in hydraulic fracturing: The Dockum Aquifer, Midland Basin, Texas, Master's thesis, University of Texas at El Paso, El Paso, Texas, 48 p.

Saller, A. H., and A. M. Stueber, 2018, Evolution of formation waters in the Permian Basin, United States: Late Permian evaporated seawater to Neogene meteoric water: AAPG Bulletin, v. 102, no. 3, p. 401–428, doi:10.1306/0504171612517157.

Scanlon, B. R., R. C. Reedy, F. Male, and M. Walsh, 2017, Water issues related to transitioning from conventional to unconventional oil production in the Permian Basin: Environmental Science & Technology, v. 51, p. 10903–10912, doi:10.1021/acs.est.7b02185.

Sofer, Z., and J. R. Gat, 1972, Activities and concentrations of oxygen-18 in concentrated aqueous salt solutions: Analytical and geophysical implications: Earth and Planetary Science Letters, v. 15, no. 3, p. 232–238, doi:10.1016/0012-821X(72)90168-9.

Sofer, Z., and J. R. Gat, 1975, The isotope composition of evaporating brines: effect of the isotopic activity ratio in saline solutions: Earth and Planetary Science Letters, v. 26, no. 2, p. 179–186, doi:10.1016/0012-821X(75)90085-0.

Spivak-Birndorf, L. J., B. W. Stewart, R. C. Capo, E. C. Chapman, K. T. Schroeder, and T. M. Brubaker, 2012, Strontium isotope study of coal utilization by-products interacting with environmental waters: Journal of Environmental Quality, v. 41, no. 1, p. 144–154, doi:10.2134/jeq2011.0222.

Stanton, J. S., D. W. Anning, C. J. Brown, R. B. Moore, V. L. McGuire, S. L. Qi, A. C. Harris, et al., 2017, Brackish groundwater in the United States: Reston, Virginia, US Geological Survey Professional Paper 1833, 185 p., doi:10.3133/pp1833.

Stueber, A. M., A. H. Saller, and H. Ishida, 1998, Origin, migration, and mixing of brines in the Permian Basin: Geochemical evidence from the eastern Central Basin Platform, Texas: AAPG Bulletin, v. 82, no. 9, p. 1652–1672.

Texas Water Development Board, 2014, Brackish resources aquifer characterization system (BRACS) database, accessed July 18, 2018, http://www.twdb.texas.gov/innovativewater/bracs/database.asp.

Texas Water Development Board, 2017, Brackish resources aquifer characterization system (BRACS), accessed September 21, 2017, http://www.twdb.texas.gov/innovativewater/bracs/index.asp.

US Energy Information Administration, 2018, Drilling productivity report, accessed February 12, 2018, http://www.eia.gov/petroleum/drilling/pdf/dpr-full.pdf.